Regulation and virulence function of *Fusarium graminearum* secondary metabolites during *Arabidopsis thaliana* infection

Marielle Zouein

Thesis submitted to the University of Ottawa

in partial fulfillment of the requirements for the
Master of Science in Biology

Department of Biology

Faculty of Science

University of Ottawa

Abstract

During plant infection, *Fusarium graminearum* induces secondary metabolite production, which include mycotoxins and virulence factors, to overcome host defenses. Different hosts can elicit expression of distinct secondary metabolite biosynthetic genes through unknown host-derived signals. Here, we investigate how the *Arabidopsis thaliana* NADPH oxidase gene *RbohD*, which contributes to stress-induced reactive oxygen species (ROS) bursts, influences fungal secondary metabolite gene expression during seedling infection. *F. graminearum* infection induces progressive accumulation of ROS in Arabidopsis cotyledons which accompanied by tissue whitening. In the fungus, 650 genes are differentially expressed during infection including 51 secondary metabolite biosynthetic genes from the trichothecene, culmorin, fusaoctaxin, butenolide and fungal decalin-containing diterpenoid pyrone clusters (FDDP). In *F. graminearum*-infected *rbohD* knockout plants, cotyledon ROS accumulation was attenuated and fungal expression of genes from the trichothecene, fusaoctaxin, butenolide, and FDDP clusters were reduced. Knocking out other host susceptibility genes, including *RLK7*, *ILK1*, and *APEX*, had no effect on ROS accumulation and impacted expression of fewer fungal secondary metabolite genes. Abolishment of fungal production of deoxynivalenol, fusaoctaxin, and FDDP reduced *F. graminearum* virulence and resulted in increased callose production in the host during infection. Together, these findings indicate that the Arabidopsis *RbohD* gene influences *F. graminearum* pathogenesis and expression of secondary metabolite virulence factors during infection.

Résumé

Pendant l'infection des plantes, *Fusarium graminearum* induit la production de métabolites secondaires, qui comprennent des mycotoxines et des facteurs de virulence, afin de surmonter les défenses de l'hôte. Différents hôtes peuvent déclencher l'expression de gènes biosynthétiques de métabolites secondaires distincts par l'intermédiaire de signaux d'origine hôte encore inconnus. Ici, nous étudions comment le gène NADPH oxydase *RbohD* d'*Arabidopsis thaliana*, qui contribue aux bouffées de production d'espèces réactives de l'oxygène (ROS) induites par le stress, influence l'expression des gènes de métabolites secondaires fongiques pendant l'infection des plantules. L'infection par *F. graminearum* induit une accumulation progressive de ROS dans les cotylédons d'Arabidopsis, accompagnée d'un blanchiment des tissus. Chez le champignon, 650 gènes sont différentiellement exprimés pendant l'infection, incluant 51 gènes biosynthétiques de métabolites secondaires provenant des clusters trichothécène, culmorine, fusaoctaxine, buténolide et pyrone diterpénoïde contenant une décaline fongique (FDDP). Chez les plantes mutantes *rbohD* infectées par *F. graminearum*, l'accumulation de ROS dans les cotylédons était atténuée, et l'expression fongique des gènes issus des clusters trichothécène, fusaoctaxine, buténolide et FDDP était réduite. L'inactivation d'autres gènes de susceptibilité de l'hôte, notamment *RLK7*, *ILK1* et *APEX*, n'a eu aucun effet sur l'accumulation de ROS et a affecté l'expression d'un plus petit nombre de gènes fongiques de métabolites secondaires. L'abolition de la production fongique de déoxynivalénol, de fusaoctaxine et de FDDP a réduit la virulence de *F. graminearum* et a entraîné une augmentation de la production de callose chez l'hôte pendant l'infection. Ensemble, ces résultats indiquent que le gène *RbohD* d'Arabidopsis influence la pathogenèse de *F. graminearum* ainsi que l'expression des facteurs de virulence liés aux métabolites secondaires pendant l'infection.

Acknowledgments

I would like to express my heartfelt gratitude to my supervisor Dr. Elizabeth Brauer for her guidance, support and patience throughout my thesis. I would like to thank my committee members Dr. David Overy and Dr. Allyson MacLean for their time and feedback.

This project would not have been possible without the guidance and assistance of colleagues at Agriculture and Agri-Food Canada. To Whynn Bosnich, who welcomed me into the lab with open arms and will always be the Brauer lab mom, thank you for your unwavering support in the lab and for the great conversations that I will forever hold in my heart. To the Brauer lab students, Emily Marion and Sid Lakshmanan, I am grateful for your friendships, moral support, and our monthly field trips, otherwise known as lunch outings. Thank you to Mirko Tabori Ortiz for training me on the infection assay protocol. Further thanks to Kristen Holy for conducting the *rbohD* and WT infection assay. I would like to thank Kasia Dadej from the MTL lab for running my RNA-seq samples. I also thank Nathan Ling for helping me get started with my RNA-seq files, and Dr. Nathaniel Zhin-Loong Lim for providing a valuable second opinion on the time course transcriptome analysis and for analyzing *rbohD* transcriptome. Further thanks to the Overy lab, especially Carmen Hicks, for running and analyzing my metabolomic samples. Finally, I thank the Subramaniam lab for their support and letting me borrow their *Fusarium* shaker on a weekly basis.

I'm extremely grateful to my parents, Elie and Liliane, and my brother Michel for their encouragement and support throughout my academic journey, especially for making my commute easier by picking me up at the train station, and for patiently enduring my thesis talk at the dinner table. Thank you for being there through the many ups and downs of my academic journey.

Table of Contents

List of Tables

List of Figures

List of Abbreviations

ABC…….ATP-binding cassette

BGC……..…….....Biosynthetic gene cluster

BUT……..Butenolide

CAZymes……..……..……...Carbohydrate-active enzymes

cDNA……...……Complementary deoxyribonucleic acid

Clm…….Culmorin

cAMP……..……..…...Cyclic adenosine monophosphate

DAB……..……Diaminobenzidine

DAMP……Damage-associated molecular pattern

DEG……...…….…….…….…..Differentially expressed gene

DNA……...…….……...Deoxyribonucleic acid

Dpi ……...…….…….Days post-inoculation

DON……...…….…….Deoxynivalenol

FDDP……..……..……Fungal decalin-containing diterpenoid pyrone

FHB……...……..…….....Fusarium head blight

ETI…….effector-triggered immunity

GAPDH……...Glyceraldehyde-3-phosphate dehydrogenase

gDNA……..Genomic deoxyribonucleic acid

GO……..……Gene ontology

H3K27me3……...…….……...Histone H3 lysine 27 trimethylation

IC……Infection cushion

ILK……...…….……..Integrin-like kinase

JA…….…Jasmonic acid

KMT6……...……..Lysine N-methyltransferase 6

MAMP…….....……...Microbe-associated molecular pattern

MAPK……..…….Mitogen activated protein kinase

MFS…….Major facilitator superfamily

NRPS……..Non-ribosomal peptide synthase

NADPH…….……Nicotinamide adenine dinucleotide phosphate

PKA……Protein Kinase A

PKS……Polyketide synthase

PTI……..……Pattern-triggered immunity

PP2A……Protein Phosphatase 2A

RbohD……..……...…Respiratory burst oxidase homolog D gene

RLK……..……..……..…….Receptor-like kinase

RNA-seq……..Ribonucleic acid sequencing

ROS……..……..……Reactive oxygen species

SA…….…Salicylic acid

TRI…….....Trichothecene genes

WT……...…….……..Wild type

qPCR……...Quantitative polymerase chain reaction

1. Introduction

1.1 Fusarium Head Blight

Fusarium species cause a variety of plant diseases such as *Fusarium* root rot, head blight and wilt (Agrios 2005). The most widely recognized of these diseases is Fusarium head blight (FHB), a fungal disease that affects several cereal crops such as wheat, barley and maize (Walter et al. 2010). FHB is caused by multiple species including *Fusarium graminearum, F. poae, F. sporotrichioides* and *F. culmorum* (Brown et al 2002; Osborne et al. 2007; Pasquali et al. 2016). Although several *Fusarium* species can cause FHB, *F. graminearum* is considered the most dangerous due to its widespread geographical distribution, aggressive infection capabilities, and extensive economic losses caused by significant reductions in grain quality and yield (Goswami et al. 2004; Leplat et al. 2013). In North America, *F. graminearum* is the predominant causal agent of FHB in wheat (Goswami et al. 2004). FHB notably reduces grain quality and yield by contaminating harvested crops with mycotoxins that pose serious health risks when consumed by humans and animals (Desjardins 2006; Pestka 2007; Miller et al. 2014). Among these mycotoxins are zearalenone, nivalenol (NIV), and deoxynivalenol (DON) (Pestka 2007; Leplat et al. 2013; Chen et al. 2019). DON is a trichothecene commonly known as vomitoxin due to its potent emetic effects and is one of the most highly regulated mycotoxins worldwide (Pestka 2007; Ekwomadu et al. 2021; Den et al. 2023). In Canada, wheat producers have reported a loss of $1.5 billion since the 1990s (Planted Firmly in Ontario's Economy 2026; Ontario Crop IPM - Wheat 2026). In Ontario, the worst case of FHB for wheat producers was in 1996 with an estimated loss of $131 million (Ontario Crop IPM - Wheat 2026). Overall, FHB caused by *Fusarium* constitutes a substantial economic burden for cereal production driven by yield losses, grain quality deterioration, and contamination with tightly regulated mycotoxins such as DON.

F. graminearum persists between growing seasons by surviving saprophytically in soil and on infected crop residues such as maize stalks and wheat straw (Leplat et al. 2013; Leplat et al. 2016). Although infection can occur in multiple plant structures such as stems, leaves, flowers and roots, floral infection has the most significant impact on grain production (Goswami et al. 2004; Keller et al. 2014). In the spring, In *F. graminearum*, asexual macroconidia are produced by conidiogenous cells called phialides, whereas sexual ascospores are produced within perithecia. (Figure 1) (Trail 2009; Leplat et al. 2013; Keller et al. 2014; Alisaac and Mahlein 2023; López-Arellanes et al. 2025). In wheat, floral infection occurs when air-borne fungal spores can enter the spikelet (seed) by colonizing the anther and the filament (Obanor et al. 2013; Keller et al. 2014; Ontario Crop IPM - Wheat 2026). If anthers have not yet emerged, spores can remain viable for several days until anthesis, then germinate and penetrate anther tissues (Ireta et al. 1994). During the early stage of infection, the fungus grows intracellularly with few or no visible symptoms (Brown et al. 2010; Qiu et al. 2019). As infection progresses, the fungus spreads through the vascular tissues, induces necrosis, and ultimately colonizes dead tissue causing spikelets to appear bleached and in severe cases, pink or black (Jansen et al. 2005; Trail 2009; Obanor et al. 2013; Keller et al. 2014). With that said, *F. graminearum* is a hemibiotroph, beginning with a brief biotrophic phase in which it depends on living host cells, followed by a necrotrophic phase in which it kills host cells and feeds on dead tissue using enzymes that degrade host cell walls (Jansen et al. 2005; De Silva 2016).

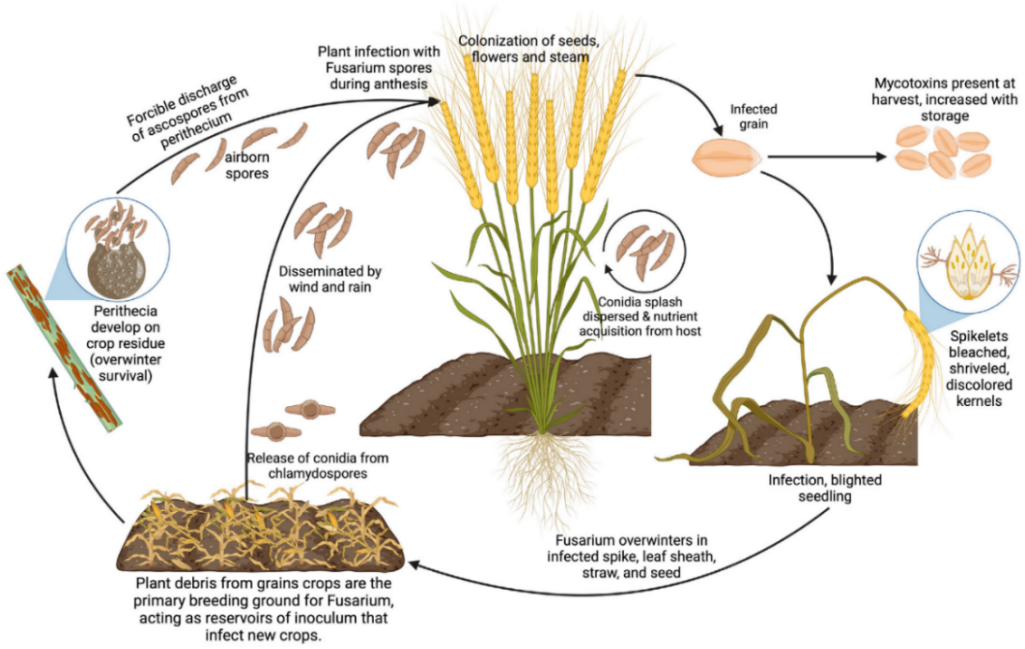

Figure 1. *Fusarium* life cycle. *Fusarium* overwinters on infected crop residues and other plant debris. Under favorable spring conditions, perithecia develop on these overwintered residues and produce asci containing sexually derived ascospores. The ascospores are forcibly discharged from the asci and released from the perithecia, dispersed by wind, and can initiate floral infection during anthesis. Asexual macroconidia may also contribute to local spread. Infection leads to colonization of spike tissues and grain, resulting in FHB symptoms and contaminated grain due to mycotoxin production (López-Arellanes et al. 2025).

During infection, the fungus produces secondary metabolites which are low-molecular-weight molecules that are not directly involved in development, growth, or reproduction but promote fungal survival under specific environmental conditions (Brakhage et al. 2013; Keller et al. 2005; Keller et al. 2019; Eagan and Keller 2025). *F. graminearum* produces numerous secondary metabolites, some of which contribute to host colonization and disease by suppressing host defences and promoting nutrient acquisition (Table 1) (Sieber et al. 2014; Adpressa et al.

2019). Enzymes involved in secondary metabolite biosynthesis are encoded by genes organized into biosynthetic gene clusters (BGCs), which are groups of two or more neighboring genes in the genome that collectively encode a biosynthetic pathway responsible for producing a specialized metabolite (Medema et al. 2015; Hoogendoorn et al. 2018; Keller et al. 2019; Rokas et al. 2020; Eagan and Keller 2025). A typical BGC contains a core synthase enzyme such as a polyketide synthase (PKS), non-ribosomal peptide synthetase (NRPS), or terpenoid synthase (TS) that assembles the backbone of the molecule (Medema et al. 2015; Hoogendoorn et al. 2018; Keller et al. 2019; Rokas et al. 2020; Eagan and Keller 2025). This scaffold is then modified by tailoring enzymes such as cytochrome P450 monooxygenases or acetyltransferase (Bills and Gloer 2016; Eagan and Keller 2025). Many BGCs encode transporters from the ABC or MFS families that export secondary metabolites into the extracellular environment (Qi et al. 2018; Eagan and Keller 2025). Finally, BGCs may contain a transcription factor that coordinates the expression of multiple genes within the cluster (Medema et al. 2015; Hoogendoorn et al. 2018; Rokas et al. 2020). The organization of BGCs makes the secondary metabolite particularly tractable in transcriptomic analyses because coordinated induction of the core synthase gene together with adjacent tailoring, transporter, and regulatory genes provides evidence for transcriptional activation of the pathway (Sieber et al. 2014; Hoogendoorn et al. 2018). Using a meta-analysis of transcriptome studies, Sieber et al. (2014) identified 67 candidate BGCs in *F. graminearum* based on co-expression and predicted enzymatic functions of genes (Sieber et al. 2014). These included the well-studied trichothecene (*TRI*) gene cluster involved in biosynthesis of DON and its acetylated derivatives, ADON and nivalenol (Brown et al. 2001; Goswami et al. 2004; Alexander et al. 2011). Other BGCs have known productions including zearalenone, the pigments aurofusarin and rubrofusarin, the terpenoid culmorin, butenolide, fusaoctaxins, and the siderophores ferricrocin, triacetylfusarinine

C, and malonichrome (Frandsen et al. 2006; Harris et al. 2007; McCormick et al. 2010; Oide et al. 2014; Sieber et al. 2014; Weber et al. 2018; Jia et al. 2019; Westphal et al. 2019). Overall, *F. graminearum* encodes many BGCs that produce diverse secondary metabolites showing chemical and biosynthetic diversity (Brakhage 2012; Sieber et al. 2014; Rokas et al. 2020).

Table 1. Examples of *F. graminearum* BGCs identified by Sieber et al. (2014) and Adpressa et al. (2019) with known metabolite product.

BCGs Number[a]	Metabolite	Function	References[b]
C02	Gramillin A/Gramillin B	Virulence factor	Bahadoor et al. (2018)
C13	Aurofusarin	Red pigment	Malz et al. (2005)
C15	Zearalenone	Powerful xenoestrogen in mammals	Gaffoor et al. (2005) & Kim et al. (2005)
C16	FDDP-D/FDDP-E		Hicks et al. (2023)
C18	Orcinol/orsellinic acid		Jørgensen et al. (2014)
C21	Triacetylfusarinine		Oide et al. (2006)
C23	Trichothecene	Virulence factor, mycotoxin	Proctor et al. (1995)
C24	Fusariumdiene/Fusagramineol		Bian et al. (2018)
C26	Gibepyrones/Prolipyrone		Westphal et al. (2018)
C28	Carotenoid		Jin et al. (2010)
C33	Ferricrocin	Siderophore	Tobiasen et al. (2006)
C42	Fusarins (fusarin A, C, D), Protofusari		Gaffoor et al. (2005)
C47	Fusaristatin A		Sørensen et al. (2014)
C48	Tricinolonoic acid, Tricinonoic acid, Tricindiol, Tricinolone		Adpressa et al. (2019); Harris et al. (2007)

C49	Butenolide		Harris et al. (2007)
C53	Perithecial Pigment, Bostrycoidins		Frandsen et al. (2016)
C59	Culmorin	Phytotoxic, antifungal	McCormick et al. (2010)
C60	Fusarielin		Sørensen et al. (2012)
C63	Malonichrome	Siderophore	Oide et al. (2014)
C64	Fusaoctaxin	Virulence Factor	Jia et al. (2019)
C66	Chrysogine	Yellow pigment	Wollenberg et al. (2017)

[a]BGCs numbering pulled from Sieber et al. (2014)

[b]References relate to the identification of metabolite.

Secondary metabolite production in *F. graminearum* is highly regulated at the transcriptional level and can depend on the environment in which the fungi is growing. Across *F. graminearum* transcriptome studies, the majority of *in planta* induced genes are expressed across infection stages, host types and tissues, with fewer genes showing host or tissue-specific expression (Boedi et al. 2016; Harris et al. 2016; Brauer et al. 2020). The status of the host however, does influence BGC expression as illustrated in a study comparing fungal expression on living versus dead wheat spikes (Boedi et al. 2016). In living spikes, *F. graminearum* expresses genes from the trichothecene, fusaoctaxin, decalin-containing diterpenoid pyrone (FDDPs), butenolide, and culmorin BGCs while these genes had lower expression during fungal infection of dead spikes (Boedi et al. 2016). These findings suggest that some BGCs are induced by signals derived from an active host environment rather than being induced by an inert nutrient source (Boedi et al. 2016). Consistent with this, multiple studies have reported induced expression during plant infection of at least twenty BGCs including clusters involved in fusaoctaxin, FDDP, DON, butenolide, and

culmorin production (Sieber et al. 2014; Boedi et al. 2016; Harris et al. 2016). Notably, C23 (trichothecene) and C64 (fusaoctaxin) clusters are upregulated in infection cushions, multicellular hyphal aggregates that are associated with penetration and localized necrotrophic growth (Choquer et al. 2020; Mentges et al. 2020). Meanwhile, the C13 cluster (aurofusarin) is upregulated only in runner hyphae and not in infection cushions (Mentges et al. 2020). Nonetheless, the tight spatial and temporal regulation of BGC expression during infection may conserve energy while ensuring that virulence factors are produced at the appropriate stage of infection and in the correct host tissues to promote fungal colonization and attack (Brakhage 2012; Keller et al. 2019).

Regulation of the BGCs induction involves multiple signals based on *in vitro* work. For the trichothecene gene cluster, *F. graminearum* induces expression in response to changes in pH, nutrient availability, plant-derived carbohydrates and stress conditions such as oxidative stress (Ponts et al. 2007; Gardiner et al. 2009; Ponts et al. 2009; Merhej et al. 2011; Montibus et al. 2013; Hou et al. 2015). For example, nonpreferred nitrogen sources and polyamine-related compounds such as agmatine are potent inducers of the *TRI* cluster and they can also induce genes involved in gramillin and culmorin biosynthesis (Gardiner et al., 2009; McCormick et al., 2010; Bahadoor et al., 2018). Within the *TRI* cluster, the transcription factors TRI6 and TRI10 coordinate expression of trichothecene biosynthetic genes, while cluster induction is further modulated by upstream signalling and nitrogen-responsive regulatory pathways (Proctor et al. 1995; Jiang et al. 2016; Hou et al. 2015). TRI6 also activates other secondary metabolite BGCs including C02 (gramillin) and C64 (fusaoctaxin) during nitrogen starvation (Nasmith et al. 2011; Jiang et al. 2016; Shostak et al. 2020). The GATA transcription factor AreA mediates ammonium- and cAMP-linked control of DON synthesis and *TRI* gene expression (Hou et al. 2015). Upstream signalling through the cAMP-PKA pathway, further regulates the *TRI* gene expression and DON production during infection (Li

et al. 2017). In *F. graminearum*, many secondary metabolite loci are associated with the repressive histone mark H3K27me3, indicating that chromatin-based silencing contributes to BGC regulation (Connolly et al. 2013). In addition, FgLaeA, a Velvet complex-associated global regulator, alters the expression of multiple BGCs in coordination with light-responsive regulatory pathways (Kim et al. 2013). Together, these findings indicate that secondary metabolite BGC expression in *F. graminearum* is tightly controlled through the integration of environmental cues, upstream signalling pathways, pathway-specific regulators, global regulators, and chromatin-based mechanisms.

During plant–pathogen interactions, secondary metabolites often function as virulence factors by suppressing host defences, promoting nutrient acquisition, and enabling pathogen growth and spread between host tissues (Brakhage et al. 2013; Eagan and Keller 2025). These virulence factors include DON, FDDPs, culmorin, gramillin, and fusaoctaxin, whose corresponding biosynthetic genes show strong *in planta* expression (Proctor et al. 1995; McCormick et al. 2010; Boedi et al. 2016; Sieber et al. 2014; Bahadoor et al. 2018; Jia et al. 2019). DON contributes to virulence in wheat by inhibiting callose production and promoting fungal spread beyond the initially infected spikelet into adjacent spikelets (Jansen et al. 2005). Culmorin is a co-occurring sesquiterpene that can potentiate DON's phytotoxic effects and has been linked to reduced DON detoxification capacity in plants, supporting a helper metabolite role during infection (Wipfle et al. 2019; Woelflingseder et al. 2019). In addition, the gramillin A and B virulence factors disrupt membrane integrity in barley to promote fungal expression of fusaoctaxin biosynthetic genes and suppress callose production in Arabidopsis (Bahadoor et al. 2018; Brauer et al. 2024). Fusaoctaxin A is a virulence factor that promotes cell-to-cell invasion of wheat that represses host callose deposition and inhibited plasmodesmatal closure during infection (Jia et al.

2019; Tang et al. 2021). The FDDPs are induced during wheat and barley infection and may promote virulence in wheat (Hicks et al. 2023). Overall, these secondary metabolite virulence factors seem to promote advancement of the fungus within the host by suppressing inducible defence (Cuzick et al. 2008; Bahadoor et al. 2018; Jia et al. 2019; Wipfle et al. 2019; Hicks et al. 2023). Fungal colonization also thought to involve proteinaceous effectors and carbohydrate-active enzymes (CAZymes) to degrade plant cell walls and support penetration, nutrient acquisition, and tissue colonization (Ferrari et al. 2012; Roy et al. 2020; Alouane et al. 2021). While the majority of these virulence factors have been established in cereal infections it remains unclear if they have a similar virulence function in Arabidopsis seedling infection.

1.2 Host recognition of *F. graminearum* and resistance

In plants, pathogen recognition can be initiated at the plasma membrane through the perception of microbe-associated molecular patterns (MAMPs) by pattern recognition receptors (PRRs) (Newman et al. 2013; Yu et al. 2017). MAMPs are conserved across a microbial group that activate pattern-triggered immunity (PTI) in plants (Newman et al. 2013; Yu et al. 2017). In addition to MAMPs, plants also perceive damage-associated molecular patterns (DAMPs), endogenous fragments released during wounding which can activate PRR-mediated immune signalling (Rubartelli and Lotze 2007; Yu et al. 2017). Whereas PTI is initiated by surface PRRs recognizing MAMPs and DAMPs, a second layer, effector-triggered immunity (ETI), is activated when intracellular immune receptors detect pathogen effectors, typically producing a stronger and more sustained defence responses (Dodds and Rathjen 2010; Yu et al. 2017). Upon PRR activation, downstream signalling is initiated including kinase phosphorylation cascades, rapid cytosolic Ca^{2+} influx and ion fluxes, transcriptional reprogramming, and the production of defence outputs such

as phytoalexins and callose production (Dodds and Rathjen 2010; Yu et al. 2017). PTI commonly involves phytohormone signalling, including salicylic acid (SA) and jasmonic acid (JA), which help coordinate defence responses appropriate to the infection context (Yu et al. 2017). One of the earliest PTI responses is the rapid generation of apoplastic reactive oxygen species (ROS), often within minutes including hydrogen peroxide (H_2O_2) (Yu et al. 2017; Fedoreyeva 2024). ROS is produced by both plasma membrane NADPH oxidases (RBOHs) and apoplastic class III peroxidases (Daudi et al. 2012; Kadota and Zipfel 2015). This oxidative burst functions in defence signalling and can promote cell wall reinforcement through oxidative cross-linking and callose deposition (Daudi et al. 2012; Rivas and Aarabi 2024).

Breeding and population-level studies has revealed that FHB resistance in cereals is quantitative and likely involves multiple genes. Researchers categorize the observed resistance types to explain differences in the speed and incidence of floral infection of wheat heads, otherwise known as spikes (Bai et al.2018; Buerstmayr et al. 2020; Buerstmayr et al., 2021; Zhang et al. 2021). For example, type I host resistance describes a lack of fungal entry into the spike, while type II resistance is restricted pathogen spread within the spike and type III resistance is the limitation of DON accumulation within an infected spike (Yan et al., 2011; Bai et al. 2018) Reduced DON accumulation may occur through detoxification, as well as through restriction of fungal colonization or disease progression (Poppenberger et al., 2003; Lemmens et al., 2005; Rivas et al., 2024). Plant resistance to *F. graminearum* may arise through physiological traits such as flowering time or induced defences triggered by DAMPs or MAMPs though in many cultivated varieties the mechanisms underlying resistance are unknown (Gunupuru et al., 2017; Sarowar et al., 2019; Buerstmayr et al., 2021; Manes et al., 2021). Host susceptibility genes also promote fungal infection, presumably because their effect on host physiology is exploited by pathogens to

promote compatibility and disease development (Lapin and Van den Ackerveken 2013). These susceptibility genes can function in processes such as pathogen establishment, suppression of host defences, or maintenance of pathogen growth, and loss-of-function can shift the interaction toward resistance (Lapin and Van den Ackerveken 2013). In wheat FHB, a clear example is the major locus *Fhb1*, where a deletion affecting the histidine-rich calcium-binding protein gene (*TaHRC*) has been shown to reduce susceptibility and confer resistance (Su et al. 2019).

Recent work on the fungal cyclic lipopeptide gramillin showed that the Arabidopsis host *ILK1* and *RbohD* genes are required for gramillin-induced stress responses and promote host susceptibility (Brauer et al. 2024). ILK1 contributes to potassium regulation across the plasma membrane during stress by stabilizing the HAK5 transporter which influences lignin formation, bacterial resistance and osmotic stress responses (Brauer et al. 2016; Dimlioglu et al. 2022) RBOHD produces a ROS burst in the apoplast in responses to multiple stresses, and is activated by kinases and calcium ions (Evans et al. 2016; Gilroy et al. 2016). RBOHD-derived ROS functions as a signal to influence cell wall reinforcement (oxidative cross-linking and callose deposition), activation of downstream defence signalling and transcriptional reprogramming, and restriction of pathogen growth at infection sites (Torres et al. 2005; Daudi et al. 2012; O'Brien et al. 2012; Morales et al. 2016; Wang et al. 2021). In Arabidopsis *rbohD* knockout mutants, leaves exhibit reduced lignin deposition in response to cell wall damage, supporting a role for ROS signalling in lignification-related cell wall remodeling (O'Brien et al. 2012). *RbohD* is also required for rapid systemic ROS signalling after localized stresses such as wounding, highlighting its role in coordinating plant immunity responses (Miller et al. 2009; Evans et al. 2016; Gilroy et al. 2016). Importantly, the disease outcome of RBOHD-derived ROS is pathosystem-dependent. For example, in the Arabidopsis–*Alternaria brassicicola* interaction, altering *RbohD* expression

affects the spatial pattern of ROS-associated cell death and has been linked to changes in fungal colonization and disease severity in specific assays (Pogány et al. 2009). In the Arabidopsis-*F. graminearum* pathosystem, fungal *TRI5* expression was almost abolished in infected *rbohD* knockout seedlings relative to wild type (WT) seedlings (Brauer et. 2024). However, fungal *TRI5* expression was unaffected in *ilk1-1* knockouts relative to the WT seedlings though both *rbohD* and *ilk1-1* plants accumulated less *F. graminearum* than the WT (Brauer et. 2014). This indicates that host factors regulate *F. graminearum* BGCs expression during infection and through either inter-species signalling or differences in fungal penetration.

1.3 Research Objectives

To better understand the role of the host in regulating *F. graminearum* BGC during infection, this thesis addresses three research objectives:

1. Establishing the expression patterns of *F. gramineaum* secondary metabolite biosynthetic genes during Arabidopsis seedling infection.
2. Assessing the influence of *RbohD* on *F. gramineaum* secondary metabolite biosynthetic gene expression and ROS production during infection.
3. Evaluating the role of *RbohD*-dependent secondary metabolites in promoting fungal virulence in Arabidopsis.

2. Methods

2.1 Arabidopsis growth conditions

Wild type *Arabidopsis thaliana* (Col-0) and Arabidopsis knockout mutants (*apex-1, rbohD, rkl7-4 and ilk1-1*) were obtained from the Arabidopsis Biological Resource Center. Arabidopsis plants were grown in Cornell soil mix in 16-hour daylight and 8-hour night at 21°C in Conviron GEN1000 chambers.

2.2 Fungal culture preparation and spore production

The *F. graminearum* WT DAOM233423 strain was provided by the Canadian Collection of Fungal Cultures at the Agriculture & Agri-Food Canada, Ottawa). The *F. graminearum* mutants *Δbut2*, *Δnrps9*, *ΔC16*, *Δtri5* and *Δfgbmh1*, as well as *F. poae* and *F. sporotrichioides* strains, were generously provided by various collaborating research groups, including Dr. Linda Harris, Dr. David Overy and Dr. Rajagopal Subramaniam at Agriculture & Agri-Food Canada. All strains were revived from -80°C glycerol stocks (15%) and cultured on synthetic nutrient agar (SNA) medium. To prepare conidia for pathogenicity assays, four 3 mm plugs was removed from the SNA plate and transferred to 50 mL of carboxymethyl cellulose medium in 250 mL Erlenmeyer flask. Cultures were incubated at 28°C with shaking at 170 rpm for 3-4 days to generate conidia. Four layers of sterile cheesecloth was used to separate mycelial solids from conidia. Conidia were washed with sterile water twice by centrifugation at 4200 rpm for 10 minutes at 4°C. Pelleted spores were resuspended in 5 mL sterile water and quantified with a hemocytometer under an optical microscope (Leica DMLB).

2.3 Arabidopsis seedling infection assay

The Arabidopsis infection assay was performed using 5-day-old seedlings grown in a 96-well plate using a previously developed protocol (Manes et al. 2021). Briefly, seeds were sterilized in 30% bleach with 0.1% Tween20 for 10 minutes and washed with sterile water three times. Six seeds were pipetted into each well of a clear 96-well plate with 100 µL liquid 1/20 Murashige and Skoog (MS) medium (2.16 g MS basal mix, 0.28 g MES monohydrate per liter of 1/2 MS liquid medium, pH 5.7). The lid of the plate was taped with micropore tape and was stratified for 2 days at 4°C. The seeds were grown for 5 days in a growth chamber at 21°C with a 16-hour daylight. Plates were tilted every other day. Before inoculation, 5-day old seedlings were washed with 0.5% sucrose and then inoculated with *F. graminearum* DAOM233423 strain, *F. graminearum* mutant strains (*Δbut2*, *Δnrps9*, *ΔC16*, *Δtri5*, *Δfgbmh1*), *F. poae*, or *F. sporotrichioides*, as appropriate for each experiment. Seedlings were inoculated with 40 spores in 50 µL of 0.5% sucrose and plates returned to the growth chamber. Cotyledon color, DAB accumulation and Trypan blue staining was observed from day 0 to day 4 dpi with a dissection microscope (Leica MZ16). To quantify fungal gene expression and biomass, cotyledons and roots were harvested from 0 to 4 dpi for the time-course experiment. For virulence assays, callose deposition, DAB staining, and analysis of Arabidopsis mutant lines seedlings were harvested at 3 dpi.

2.4 RNA extraction and quantitative real-time PCR

For analysis of fungal secondary metabolite gene expression by real-time quantitative PCR (qRT-PCR), Arabidopsis seedlings inoculated with *F. graminearum* DAOM233423 strain were harvested at 0, 1, 2, 3, and 4 dpi for the time-course experiment and at 3 dpi for all other assays. Seedlings were flash-frozen in liquid nitrogen and ground to a fine powder using a chilled mortar

and pestle. Total RNA was extracted using the RNeasy Mini Kit (Qiagen) with on-column DNase I treatment (Qiagen, Mississauga, Canada), following the manufacturer's instructions. Complementary DNA (cDNA) was synthesized from purified RNA using the High-Capacity cDNA Reverse Transcription Kit (Applied Biosystems, Thermo Fisher Scientific). qRT-PCR reactions were performed using the Power SYBR Green Master Mix (Applied Biosystems, Thermo Fisher Scientific). Amplification conditions consisted of an initial denaturation at 95°C for 15 seconds, annealing at 60°C for 15 seconds, and extension at 72°C for 1 minute, repeated for 40 cycles. Relative expression levels were calculated using standard curves generated for each primer set. Fungal gene expression was normalized using to *F. graminearum* reference genes *GAPDH (FGSG_16627)* and *β-tubulin (FGSG_09530)*, while Arabidopsis *PP2A (AT1G69960)* and *β*-Tubulin *(AT4G14960)* were used for plant normalization. Primer sequences are listed in Supplemental Table S1.

2.5 DNA Extraction and quantitative real-time PCR

To quantify fungal biomass in infected Arabidopsis seedlings, genomic DNA (gDNA) was extracted from frozen seedlings in an extraction buffer (20 mM Tris-HCl, 250 mM NaCl, 25 mM EDTA, 0.5% SDS). Samples were homogenized using the FastPrep-24™ Classic bead beating grinder and lysis system (MP Biomedicals) with sterile metal beads. Following homogenization, the lysate was centrifuged at 13000 rpm for 5 minutes. A volume of 300 µL of the supernatant was transferred to a new tube and mixed with 300 µL of isopropanol by gentle inversion. DNA was pelleted by centrifugation at 13000 rpm for 10 minutes, washed with 500 µL of 70% ethanol, and air-dried. The DNA pellet was resuspended in 80 µL of sterile distilled water. Quantitative PCR was performed using the PowerUp SYBR Green Master Mix (Applied Biosystems, Thermo Fisher

Scientific) with an initial denaturation at 95°C for 15 seconds, annealing at 60°C for 15 seconds, and extension at 72°C for 1 minute, and repeated for 40 cycles. Relative fungal DNA levels were calculated using standard curves generated for each primer pair. Gene expression was normalized to *F. graminearum* reference genes *GAPDH (FGSG_16627)* and *β-tubulin (FGSG_09530)*, while Arabidopsis *PP2A (AT1G69960)* and *BIK1 (AT2G39660)* were used for plant expression. Primer sequences are listed in Supplemental Table S1.

2.6 Secondary metabolite quantification

Infected Arabidopsis seedlings were harvested 4 days after infection with the indicated *F. graminearum* strain to evaluate fungal metabolite accumulation. Four replicate samples were gathered per strain containing 60 seedlings which were harvested from 10 wells (6 seedlings per well) from the 96-well plate infection setup described above. Seedlings and the surrounding infection liquid were collected into separate 2 mL tubes. The infection liquid was dispensed into labeled Virtuoso SureStop 2 mL amber vials and dried to completion in a Genevac evaporator for 2 hours, after which dried vials were stored at -20°C. Frozen seedlings were homogenized by adding a single metal bead to each tube and grinding in a ball mill for 5 minutes, then extracted by adding 350 µL acetonitrile containing 0.1% formic acid (with the bead retained in the tube), gently mixing, and rotating on a rotary mixer for 2 hours. Extracts were then centrifuged at 6000 rpm for 5-8 minutes to pellet debris, and 150 µL of extraction solvent was transferred into labeled 2 mL amber vials, followed by 5 minutes sonication (Fisher Scientific FS30D Ultrasonic Cleaner), and the clarified extract was transferred into HPLC vial inserts. Extracts were submitted to a collaborating lab (Dr. David Overy lab) for analysis and annotation of known *F. graminearum* secondary metabolites.

2.7 Callose staining & quantification

Callose deposition was assessed by aniline blue staining and fluorescence microscopy as previously described (Schenk and Schikora 2015). Five-day-old Arabidopsis seedlings were inoculated with *F. graminearum* DAOM233423 strain or knockout mutant strains (*Δfgm5, ΔC16, Δtri5*, *Δfgbmh1)*. Infected seedlings were harvested at 3 dpi and fixed in 1:3 (v/v) acetic acid:ethanol overnight until tissue was transparent. Samples were washed in 150 mM K_2HPO_4 for 30 min and incubated for 2 hours in staining solution containing 150 mM K_2HPO_4 and 0.01% (w/v) aniline blue, protected from light. Stained seedlings were mounted in 50% glycerol and examined using a Zeiss Axio Imager M2 fluorescence microscope with a DAPI filter. Callose deposits were quantified by manual counting across both cotyledons of each seedling. For each experiment, at least six seedlings were analyzed per technical replicate, and a minimum of three independent experiments were performed.

2.8 Diaminobenzidine staining & quantification

Hydrogen peroxide (H_2O_2) accumulation was assessed by 3,3'-diaminobenzidine (DAB) as previously described (Daudi and O'Brien 2012). DAB staining was used to localize ROS in Arabidopsis tissue inoculated with *F. graminearum* DAOM233423 strain harvested at 3 dpi. A DAB staining solution of 1 mg/mL was prepared by dissolving 50 mg of DAB in 45 mL sterile water. The solution was adjusted to a pH of 3.0 using 0.2M HCl. Next, 25 µL Tween20 and 2.5 mL of 200 mM Na2HPO4 were added for a final concentration of 10 mM Na2HPO4. Arabidopsis seedlings were stained with DAB and a gentle vacuum was used for 5 minutes to enhance uptake

of DAB and then left at room temperature in the dark on a shaker for 4-5 hours at 80-100 rpm. After incubation, DAB solution was removed and replaced with a bleaching solution (ethanol: acetic acid: glycerol, 3:1:1). The samples were heated in an oven at 90-95°C for 30 minutes to bleach out the chlorophyll. After 30 minutes, old bleaching solution was removed and replaced with fresh bleaching solution and stored at 4°C until imaging using Zeiss Axio Imager M2 Brightfield. For quantification, DAB staining was scored visually as a binary phenotype where 0 = no visible brown precipitate and 1 = visible brown precipitate in cotyledon, stem, root tip and full root.

2.9 Trypan blue staining & quantification

Trypan blue staining was used to assess plant cell death in Arabidopsis tissue inoculated with *F. graminearum* DAOM233423 strain and harvested at 3 dpi. The trypan blue staining stock consisted of 500 g phenol dissolved in 500 mL water, 500 mL lactic acid, 500 mL glycerol, and 1 g trypan blue, mixed until fully dissolved and homogeneous. A fresh working solution was prepared by mixing 1 part staining stock with 2 parts 95–100% ethanol (v/v) (for example, 3.3 mL stock and 6.7 mL ethanol to make 10 mL working solution). Samples were fully submerged in the working stain solution in 2 mL tubes. The tubes were placed in a heat block at 90 °C for 3 min and then left at room temperature for 5 min. The stain was removed and replaced with chloral hydrate destaining solution prepared by dissolving 250 g chloral hydrate in 200 mL water, and samples were cleared on an orbital rotator until the tissue became transparent. The chloral hydrate solution was replaced if it became dark blue. After destaining, tissues were transferred to 50% glycerol for 30 min, mounted on slides, and imaged by brightfield microscopy using a Zeiss Axio Imager M2.

For quantification, cell death was scored across the cotyledon only using a binary scheme: 0 = no blue staining (no detectable cell death) and 1 = blue staining present (cell death).

2.10 RNA-seq analysis

For RNA-seq analysis, *F. graminearum* DAOM233423 strain inoculated Arabidopsis seedlings were harvested at 0, 1, 2, 3, and 4 dpi with 3 or 4 replicate samples per timepoint. Total RNA quality was assessed using RNA ScreenTape on the 4200 TapeStation system (Agilent Technologies). Samples with RNA integrity number (RIN) values ≥ 5 were selected for mRNA library preparation. For library construction, 300 ng of RNA was used per sample; however, sample ArabFg2024_3DPI_R1 was normalized to 240 ng and ArabFg2024_4DPI_R1 to 120 ng. Each RNA sample was spiked with 90 pg, 72 pg, or 36 pg of Spike-In RNA Variant (SIRV) Set-2 Iso Mix E0 (Lexogen), following the SIRVs User Guide. Polyadenylated RNA was enriched using poly-T–coated magnetic beads according to the Lexogen Poly(A) RNA Selection Kit protocol. The isolated mRNA was used to construct libraries with the CORALL-V2 Library Prep Kit (Lexogen). Unique Dual Indexes (UDIs, Set-B1) were added during 12 cycles of PCR amplification following the RTM (Short Insert Size) protocol. Final libraries were evaluated using D5000 ScreenTape on the TapeStation 4200 system, revealing an average fragment size of approximately 380 bp. Library concentrations were determined using the Qubit High Sensitivity dsDNA Assay (Thermo Fisher Scientific), and equimolar amounts were pooled for sequencing. Sequencing was performed on an Illumina NextSeq 500 using the High Output Reagent Kit v2 (150 cycles), generating paired-end reads according to the manufacturer's recommendations. Raw read quality was assessed using Sequencing Analysis Viewer (Illumina) and FastQC. The *F. graminearum* PH-1 reference genome and annotation were obtained from FungiDB (Cuomo et al. 2007; Basenko et al. 2018). To analyze

fungal gene expression, reads were aligned to the reference genome using STAR v2.7.10a with default parameters (Dobin et al. 2013). Genome annotation was converted from GFF3 to GTF format using AGAT v0.9.1. Reads aligning to each gene were quantified using the GeneCounts function in STAR. Differential expression analysis was conducted in R v4.3.2 using the edgeR package v4.0.16 (Robinson et al. 2010; R Core Team 2013). Low expressed genes were filtered using edgeR's filterByExpr() function with default parameters, which applies a counts-per-million-based expression threshold; in this dataset, genes were required to be expressed above the threshold in at least the minimum group size of three samples. Library sizes were normalized using edgeR's default TMM normalization method. Differential expression was assessed using generalized linear models with quasi-likelihood F-tests. Differentially expressed genes were identified from pairwise comparisons of day 2 vs day 1, day 3 vs day 1, and day 4 vs day 1. Significant genes were defined as those with an absolute log2 fold change > 1 and a false discovery rate (FDR) < 0.05. Differentially expressed genes were submitted separately to g:Profiler for Gene Ontology (GO) enrichment analysis using default parameters (Kolberg et al. 2023).

2.11 Statistical analyses

Statistical analyses were performed using Excel and R. Gene expression, fungal biomass, and colony growth data were analyzed using one-tailed Student's t-tests. Callose deposition values were analyzed by one-way ANOVA followed by Dunnett's multiple-comparisons test to compare each *F. graminearum* mutant with the WT control. Categorical outcomes from DAB staining (H_2O_2 accumulation) and trypan blue staining were analyzed using chi-square tests. For all analyses, $p<0.05$ was considered statistically significant. All experiments were performed three times unless

otherwise specified with similar results, and the significance symbol (*) is defined in the corresponding figure legends.

3. Results

3.1 Arabidopsis seedling-*F. graminearum* interactions and secondary metabolite gene expression

To evaluate *F. graminearum* infection in Arabidopsis seedlings, we observed the daily progression of disease symptoms and ROS accumulation in seedlings over 4 days after inoculation (Figure 2A, B). Seedling cotyledons were green at 1 dpi and started showing signs of bleaching at the hydathode at 2 dpi which became more pronounced across the cotyledon at 3 dpi (Figure 2A, B). This corresponded with punctate ROS accumulation in cotyledons starting at 2 dpi and peaking at 3 dpi (Figure 2A, B). The entire cotyledon became pale green or completely bleached by 4 dpi which corresponded with substantially higher fungal growth and reduced ROS accumulation as seedlings died (Figure 2). While ROS production was also observed in the root cortex and root tip, ROS accumulation was the same between infected and uninfected plants and is thus independent of *F. graminearum* interactions (Figure 3). To determine if other plant-associated *Fusarium* species had a similar effect on Arabidopsis, we inoculated seedlings with *F. poae* and *F. sporotrichioides* which both cause FHB in crops, though are typically considered to be less virulent. *F. sporotrichioides* and *F. poae* induced cotyledon whitening more slowly than *F. graminearum* within 6 and 5 dpi, respectively (Figure 4A). This corresponded with a lower abundance of *F. poae* biomass relative to *F. graminearum* at 3 dpi (Figure 4B).

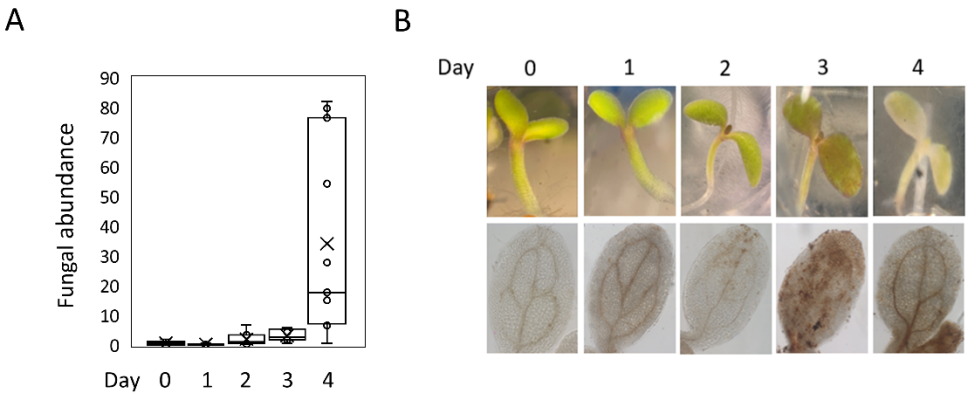

Figure 2. *F. graminearum* infection causes ROS accumulation which corresponds to symptom development and fungal gene expression. A) Fungal abundance was measured in Arabidopsis WT Col-0 seedlings infected with *F. graminearum* DAOM233423 strain at 3 dpi (n=4). Fungal abundance was measured using qPCR on cDNA by dividing the average of fungal housekeeping genes (*GAPDH, Fg β-tubulin*) by plant housekeeping genes (*Plant β-tubulin, PP2A*). The experiment was repeated three times. The data from all experiments is plotted here. B) Representative images of Arabidopsis WT Col-0 seedlings showing visible symptoms development on cotyledons and progression of ROS accumulation over 4 dpi. ROS was visualized by DAB staining for H_2O_2. Visible tissue damage was shown in cotyledon browning and whitening became more visible on 3 and 4 dpi, respectively. The experiment was repeated three times with similar results.

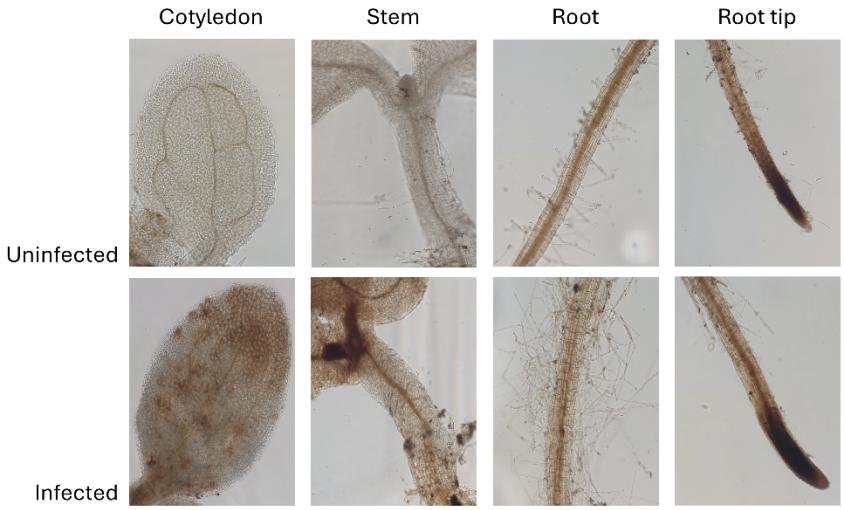

Figure 3. H_2O_2 accumulates in Arabidopsis seedling stems and cotyledons during *F. graminearum* infection. Representative photos taken of Arabidopsis WT Col-0 seedlings 3 dpi with *F. graminearum* DAOM233423 strain (inoculated) or 0.5% sucrose (uninfected), stained with DAB to visualize H_2O_2 accumulation. Fungal infection increases the amount of DAB staining in the cotyledon and stem vascular tissue. Similar results were visualized in 5 independent experiments with a minimum of 18 seedlings per experiment.

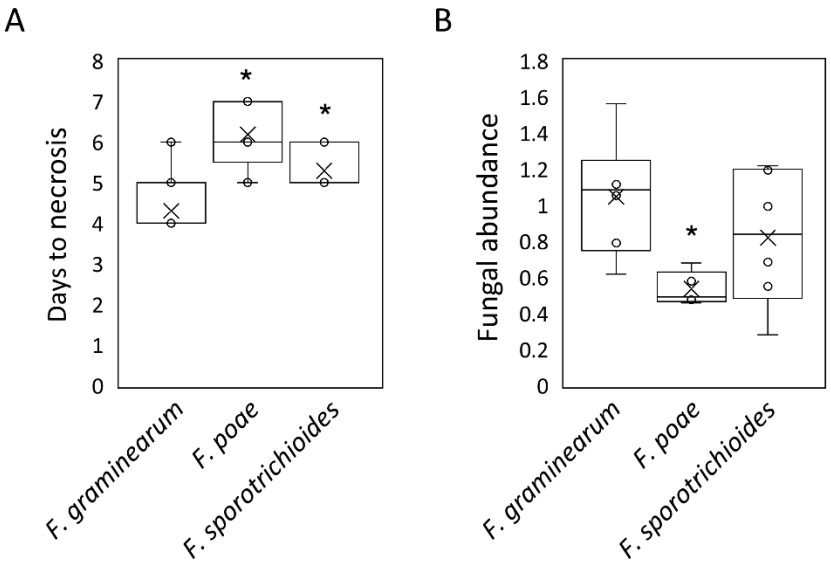

Figure 4. *F. poae* and *F. sporotrichioides* have reduced symptomology and fungal abundance in comparison to *F. graminearum*. A) The box plot represents the number of days before necrosis (seedling turning white) for each *Fusarium* species. Arabidopsis WT Col-0 seedlings 3 dpi where cotyledon symptoms were scored per seedling using binary scale (1= green, 2 = white). An asterisk (*) indicates a statistically significant difference determined by one-tailed t-test ($p<0.05$). The experiment was repeated three times with similar results. The data from all experiments is plotted here. B) The box plot represents fungal biomass in Arabidopsis WT Col-0 seedlings inoculated with *F. graminearum* DAOM233423 strain, *F. poae* and *F. sporotrichioides* at 3 dpi (n=6). Fungal biomass was measured using qPCR on gDNA by dividing the average of fungal housekeeping genes (*GAPDH, Fg β-tubulin*) by plant housekeeping genes (*Plant β-tubulin, PP2A*). An asterisk (*) indicates a statistically significant difference determined by one-tailed t-test ($p<0.05$). The experiment was repeated twice with similar results. The data from one experiment is plotted here.

To capture the dynamics of *F. graminearum* expression within this Arabidopsis seedling-*F. graminearum* pathosystem, we performed a time course RNA-seq analysis from 0 to 4 dpi. An increasing number of differentially expressed genes (DEGs) were identified over 2-4 dpi relative to 1 dpi with a total of 2309 DEGs identified (Figure 5A, Supplemental Data 1A-C). Overall, these DEGs were enriched in genes with putative roles in small molecule metabolism and carbohydrate metabolism including CAZymes (Figure 5B, Supplemental Data D-F). There were 650 DEGs which were shared across time points and were enriched for genes associated with oxidoreductase and catalytic activity (Supplemental Data 1G). Within this set of shared genes, 51 genes belonged to secondary metabolite BGCs included several genes from the C23 (trichothecene), C59 (culmorin), C64 (fusaoctaxin), C49 (butenolide), C16 (FDDP), C13 (aurofusarin) and C18 (orcinol) clusters (Supplemental Data 1H). Similar trends in secondary metabolite gene expression were observed using qPCR (Figure 6). In addition, 1989 genes were uniquely expressed at 4 dpi including genes with putative roles in primary metabolism, transport, stress response, secondary metabolism, and CAZymes (Figure 5C). These included 49 secondary metabolite genes from BGCs including the C02 (gramillin) and C9, C18 (orcinol), C26 (gibepyrones), C28 (carotenoid), C33 (ferricrocin), C38, C59 (culmorin) and C62 BGCs (Supplemental Data 1J). In addition, day 4 specific genes also included multiple CAZymes consistent with fungal cell wall remodeling and host polymer degradation, including β-1,3-glucanases and related enzymes (*FGSG_00314, FGSG_01250, FGSG_02807, FGSG_06119*), chitin-associated enzymes (*FGSG_00173, FGSG_03017, FGSG_03212, FGSG_03591, FGSG_05847*), and plant cell wall starch-degrading activities such as β-glucosidases and polysaccharide hydrolases (*FGSG_00767, FGSG_03570, FGSG_06605, FGSG_07551, FGSG_03842*) (Supplemental Data 1J). Collectively, these results show that symptom development corresponds with fungal abundance and transcriptional

reprogramming, where some BGCs are expressed throughout infection while others were detected when during host death when fungal biomass was high.

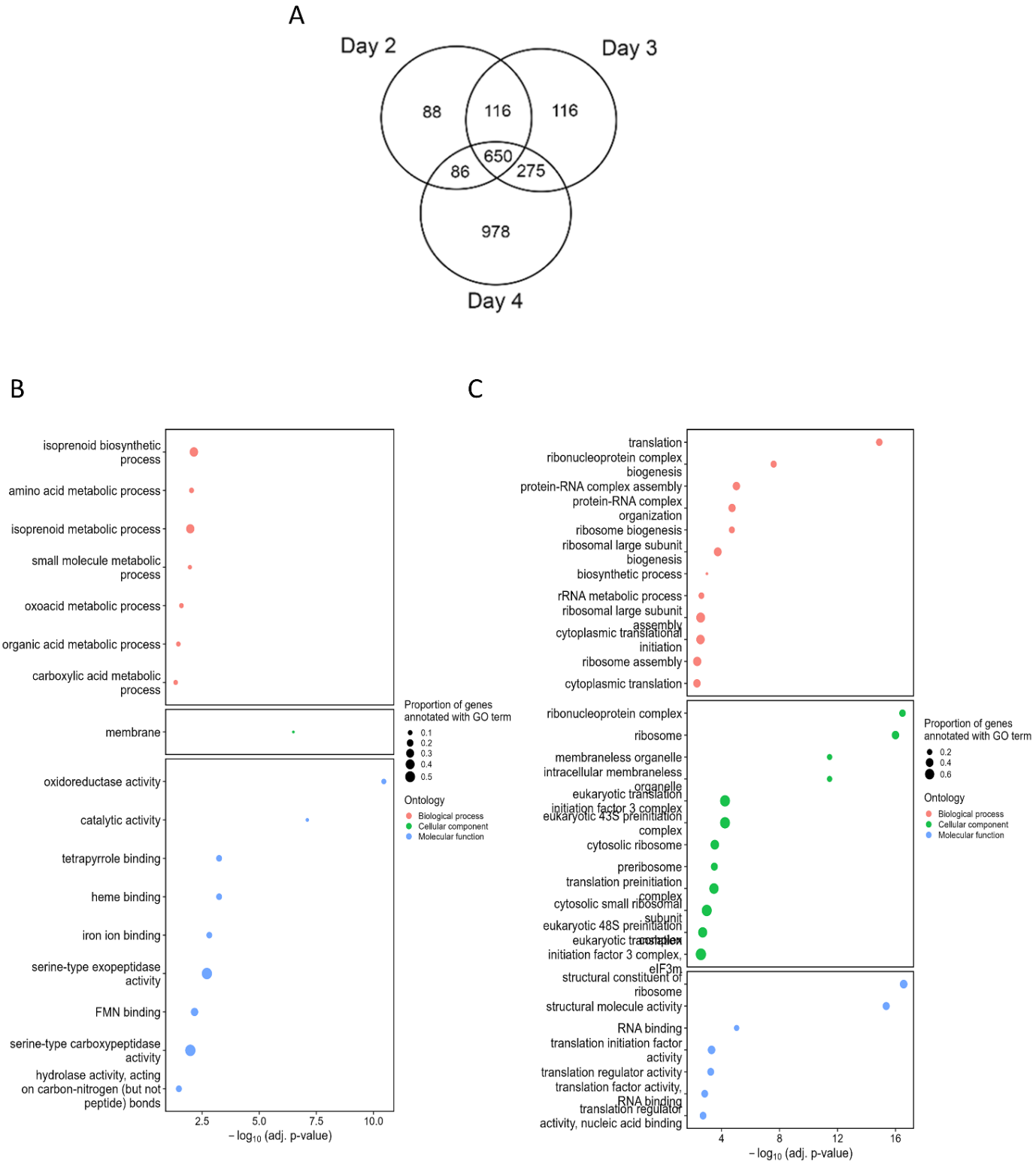

Figure 5. Time course DEGs overlap identifies a shared infection program enriched for oxidoreductase, catalytic activity and secondary metabolism. A) Venn diagram showing the

overlap of differentially expressed genes (DEGs) identified at each time point during the *F. graminearum* time course in inoculated Arabidopsis seedlings (1–4 dpi), with comparisons made relative to 1 dpi (n = 4). Each circle represents up- and downregulated fungal DEGs at each time point (|logFC| > 1, FDR < 0.05). The experiment was performed once. B) Bubble plot summarizing significantly enriched GO for the 650 DEGs found in 2-4 dpi. DEGs were separately submitted to g:Profiler for GO enrichment using default parameters (Kolberg et al. 2023). The x-axis indicates enrichment significance as −log10(adjusted p-value) and the y-axis lists enriched GO terms. Bubble size represents the proportion of genes annotated with each GO term, and bubble colour denotes GO ontology (biological process=red, cellular component=green, molecular function=blue). Terms are displayed in stacked BP/CC/MF panels separated by borders. Only significantly enriched terms (adjusted p<0.05) are shown. C) Bubble plot summarizing significantly enriched GO for the 978 DEGs found exclusively on 4 dpi. DEGs were separately submitted to g:Profiler for GO enrichment using default parameters (Kolberg et al. 2023). The x-axis indicates enrichment significance as −log10(adjusted p-value) and the y-axis lists enriched GO terms. Bubble size represents the proportion of genes annotated with each GO term, and bubble colour denotes GO ontology (biological process=red, cellular component=green, molecular function=blue). Terms are displayed in stacked BP/CC/MF panels separated by borders. Only significantly enriched terms (adjusted p<0.05) are shown.

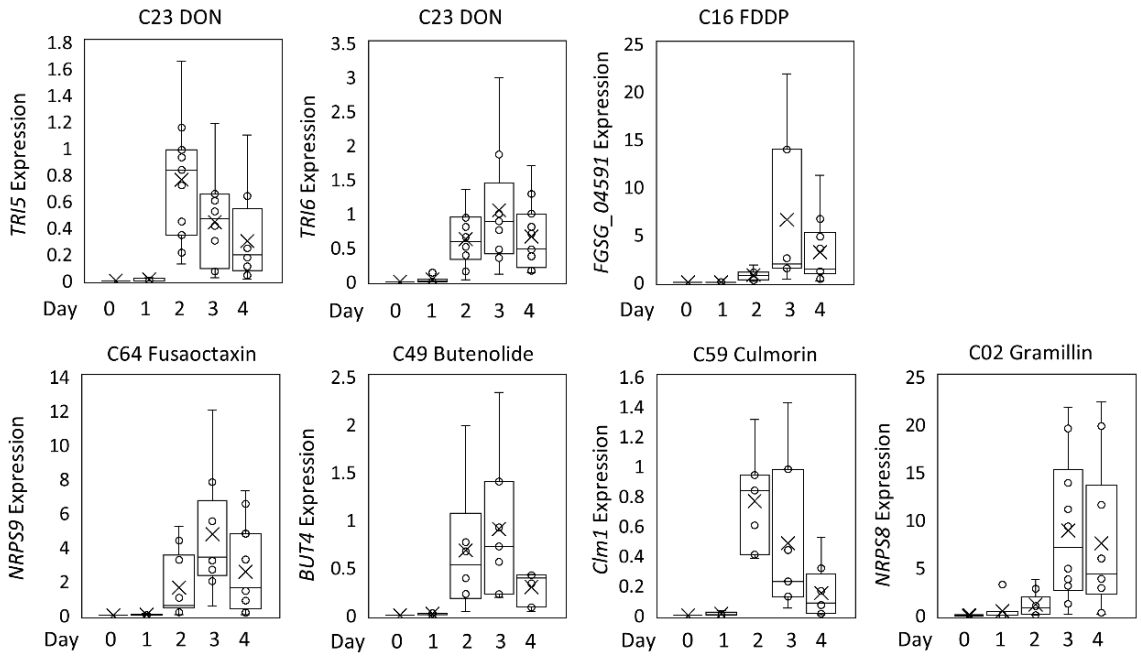

Figure 6. Expression level of key fungal secondary metabolite time course of Arabidopsis **seedlings infection of *F. graminearum*.** The box plots represent the ratio of fungal gene expression relative to fungal housekeeping genes (*GAPDH, Fg β-tubulin*). Arabidopsis WT Col-0 seedlings inoculated with *F. graminearum* DAOM233423 strain were harvested at 0, 1, 2, 3, and 4 dpi (n = 4). The experiment was repeated three times with similar results. The data from all experiments is plotted here.

3.2 The Arabidopsis *RbohD* susceptibility gene promotes H_2O_2 accumulation and virulence factor expression

Previous work has shown that the Arabidopsis *RbohD* gene promotes expression of the *F. graminearum TRI5* and *NRPS9* genes at 3 dpi (Brauer et al. 2024). We observed that at 3 dpi, the H_2O_2 accumulation in *F. graminearum* infected *rbohD* knockout mutant cotyledons was almost completely abolished relative to WT cotyledons (Figure 7, Supplemental Table S2). Punctate

lesions of dead cells were apparent in both WT and *rbohD* cotyledons indicating that *F. graminearum* was penetrating both genotypes (Figure 7, Supplemental Table S3). The *F. graminearum* NADPH oxidase-transcribing *FgNoxA* and *FgNoxB* genes had no impact on H_2O_2 accumulation in the cotyledon (Supplemental Table S2).

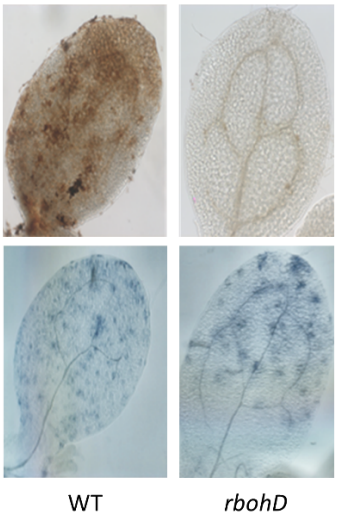

Figure 7. H_2O_2 production in *F. graminearum*-infected Arabidopsis cotyledons is dependent on the host *RbohD* gene. In the top panel visualization of H_2O_2 production in Arabidopsis WT and *rbohD* mutant cotyledons was done by DAB staining after inoculation with *F. graminearum* DAOM233423 strain for 3 days. ROS accumulated in 3 out of 48 *rbohD* seedlings and 66 out of WT 68 seedlings (Supplemental Table S2). In the lower panel cell death was visualized in Arabidopsis cotyledons by trypan blue staining in the same samples as described in the top panel. Cell death was found in 36 out of 42 *rbohD* cotyledons and 54 out of 55 WT cotyledons (Supplemental Table S3). The experiment was repeated twice with similar results.

To determine the impact of *RbohD* on *F. graminearum* gene expression, we conducted transcriptome profiling on fungal expression in infected *rbohD* knockout seedlings compared to WT seedlings at 3 dpi. In infected *rbohD,* 712 F. *graminearum* genes were differentially expressed relative to infection of WT seedlings. Of these, 567 were upregulated and 145 were downregulated in *rbohD* relative to WT (Supplemental Data 2A,B). The 145 fungal genes with lower expression in *rbohD* relative to WT seedlings included the *TRI5* and *NRPS9* as expected, as well as 40 BGC genes primarily in the C64 (fusaoctaxin), C49 (butenolide), C23 (trichothecene) and C16 (FDDP) clusters (Figure 8A, Supplemental Data 2B). The 145 DEGs were also enriched in carbohydrate catabolic genes including 31 CAZymes (Supplemental Data 2C-E). The fungal genes with higher expression in *rbohD* seedlings relative to WT seedlings are enriched in transmembrane transport and transporter activity (Supplemental Data 2C-E). Therefore, *RbohD* influences the expression of approximately 1% of *F. graminearum* genes during Arabidopsis seedling infection which include several secondary metabolite biosynthetic genes, CAZymes and transporter-encoding genes.

To determine whether *RbohD*-dependent fungal secondary metabolites are important for pathogenesis, we assessed the virulence of fungal mutants lacking DON (*Δtri5*), fusaoctaxin (*Δfgm5*), butenolide (*Δbut2*) or FDDP (*ΔC16*) production relative to a *F. graminearum* DAOM233423 strain (Figure 8A). Disruption of DON, fusaoctaxin, and FDDP production in *Δtri5*, *Δfgm5*, and *ΔC16* was validated by metabolomic analysis, while reduced butenolide expression in the *Δbut2* strain was validated by qPCR (Supplemental Figure S1). After 3 dpi, *Δbut2* mutant grew to the same extent as the *F. graminearum* DAOM233423 strain in WT plants. However, the *Δtri5, Δfgm5*, and *ΔC16* strains had reduced fungal growth relative to the WT (Figure 8A). Infection with Δ*fgm5,* Δ*C16* or Δ*tri5* corresponded with increased callose deposition

in the host compared to infection with the WT strain (Figure 8B). All mutant strains displayed typical growth in solid media suggesting their lack of growth in the plant is not due to a growth defect (Supplemental Figure S2). This indicates that DON, fusaoctaxins, and FDDPs function as virulence factors during Arabidopsis seedling infection and that their production suppresses callose deposition in the host.

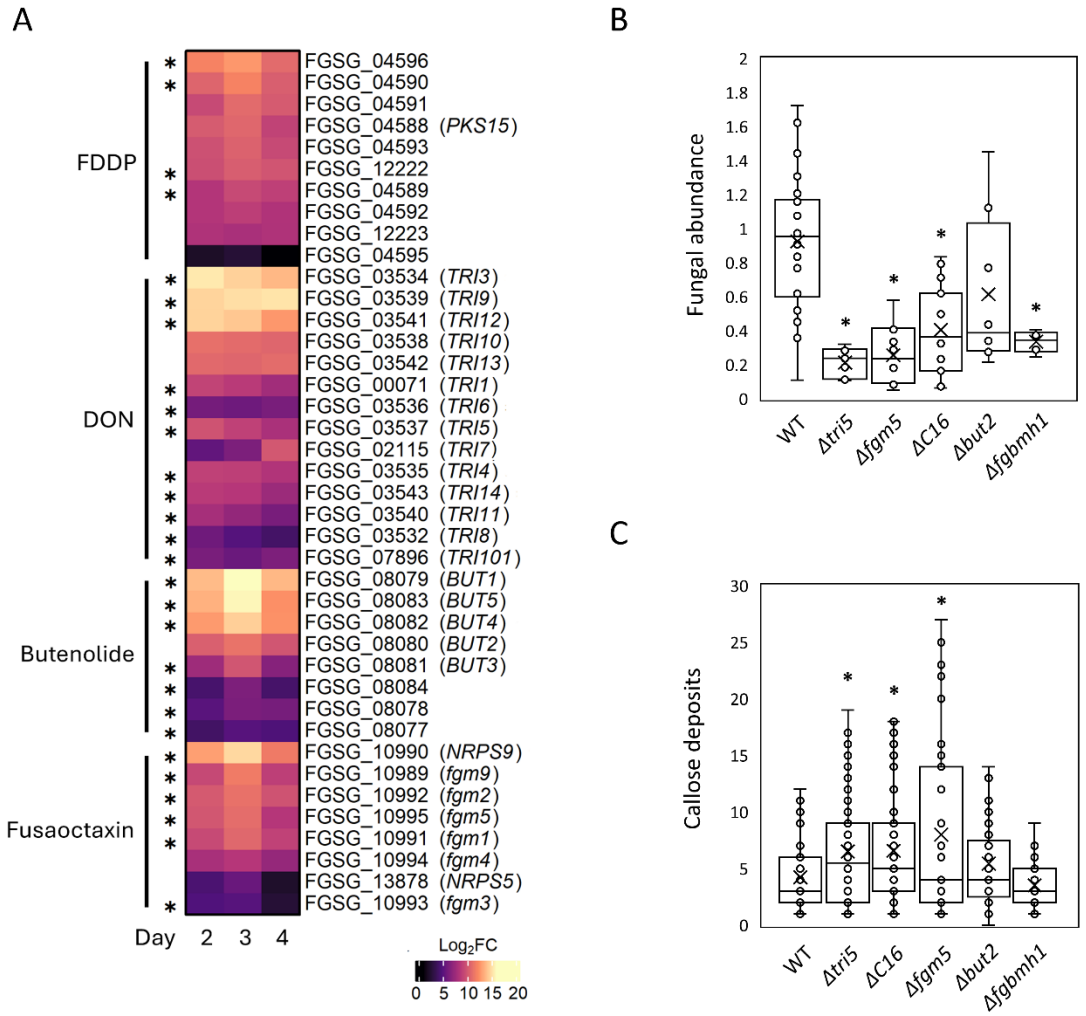

Figure 8. The Arabidopsis host *RbohD* expression influences fungal secondary metabolite gene expression, where some secondary metabolites promote virulence and suppress host callose deposition. A) Heatmap indicates relative expression of four secondary metabolite BGCs at 2, 3 or 4 dpi relative to 1 dpi (n=4). Asterisks (*) indicate genes that were significantly downregulated in fungal transcripts recovered from infected *rbohD* seedlings relative to WT seedlings in a separate RNA-seq experiment using Arabidopsis seedlings inoculated with *F. graminearum* DAOM233423 strain and harvested at 3 dpi. The experiment was repeated once. The *TRI* genes annotations were based on Hao et al. (2014). B) Fungal biomass was measured in

Arabidopsis WT Col-0 seedlings inoculated with *F. graminearum* DAOM233423 strain (WT) and *F. graminearum* mutants (Δ*but2,* Δ*fgm5,* Δ*C16,* Δ*tri5,* Δ*fgbmh1*). Seedlings were harvested at 3 dpi (n=4). Fungal biomass was measured using qPCR on gDNA by dividing the average of fungal genes (*GAPDH, Fg β-tubulin*) by average of plant genes (*PP2A, BIK1*). An asterisk (*) indicates a statistically significant difference determined by one-tailed t-test ($p<0.05$). The experiment was repeated three times with similar results. The data from all experiments is plotted here. C) Callose deposition in Arabidopsis WT seedlings 3 dpi with *F. graminearum* DAOM233423 strain (WT) and *F. graminearum* mutants (Δ*but2,* Δ*fgm5,* Δ*C16,* Δ*tri5,* Δ*fgbmh1*). Callose was visualized by fluorescence microscopy following aniline blue staining and quantified as callose deposits per cotyledon (points represent individual cotyledon). Data shown as mean ± SD (n = 43-85) seedlings per genotype. An asterisk (*) indicates a statistically significant difference determined by one-way ANOVA with Dunnett's post-hoc test ($p<0.05$). The experiment was repeated three times with similar results. The data from all experiments is plotted here.

3.3 Host susceptibility genes have differential contributions to fungal gene expression

To determine whether other host susceptibility genes influence *F. graminearum* secondary metabolite gene expression, we compared H_2O_2 accumulation and fungal expression in Arabidopsis knockout lines *apex1-1, rlk7-4, ilk1-1,* and *rbohD* at 3 dpi to WT plants (Manes et al. 2021; Brauer et al. 2024). Among these genotypes, only the *rbohD* mutant showed reduced H_2O_2 during infection (Figure 9A, Supplemental Table S2). For the fusaoctaxin cluster, fungal *fgm5* transcript abundance was significantly reduced during infection of *rbohD* plants relative to WT, while fungal *NRPS9* transcript abundance was significantly reduced in all Arabidopsis mutant lines except *rlk7-4* (Figure 9B). For trichothecene genes, *TRI3* and *TRI9* expression was reduced in

rbohD and *rlk7-4* mutants or *rbohD* and *ilk1-1*, respectively, plants relative to WT plants (Figure 9B). In addition, the culmorin biosynthetic gene *Clm1* had reduced expression in *rbohD, apex1-1* and *rlk7-4* mutants relative to the WT plants. In contrast, expression of the FDDP and butenolide biosynthetic genes were not altered across the plant lines. Collectively, these results indicate that the *rbohD* mutant exhibited the strongest effects on both host H_2O_2 accumulation and fungal secondary metabolite gene expression.

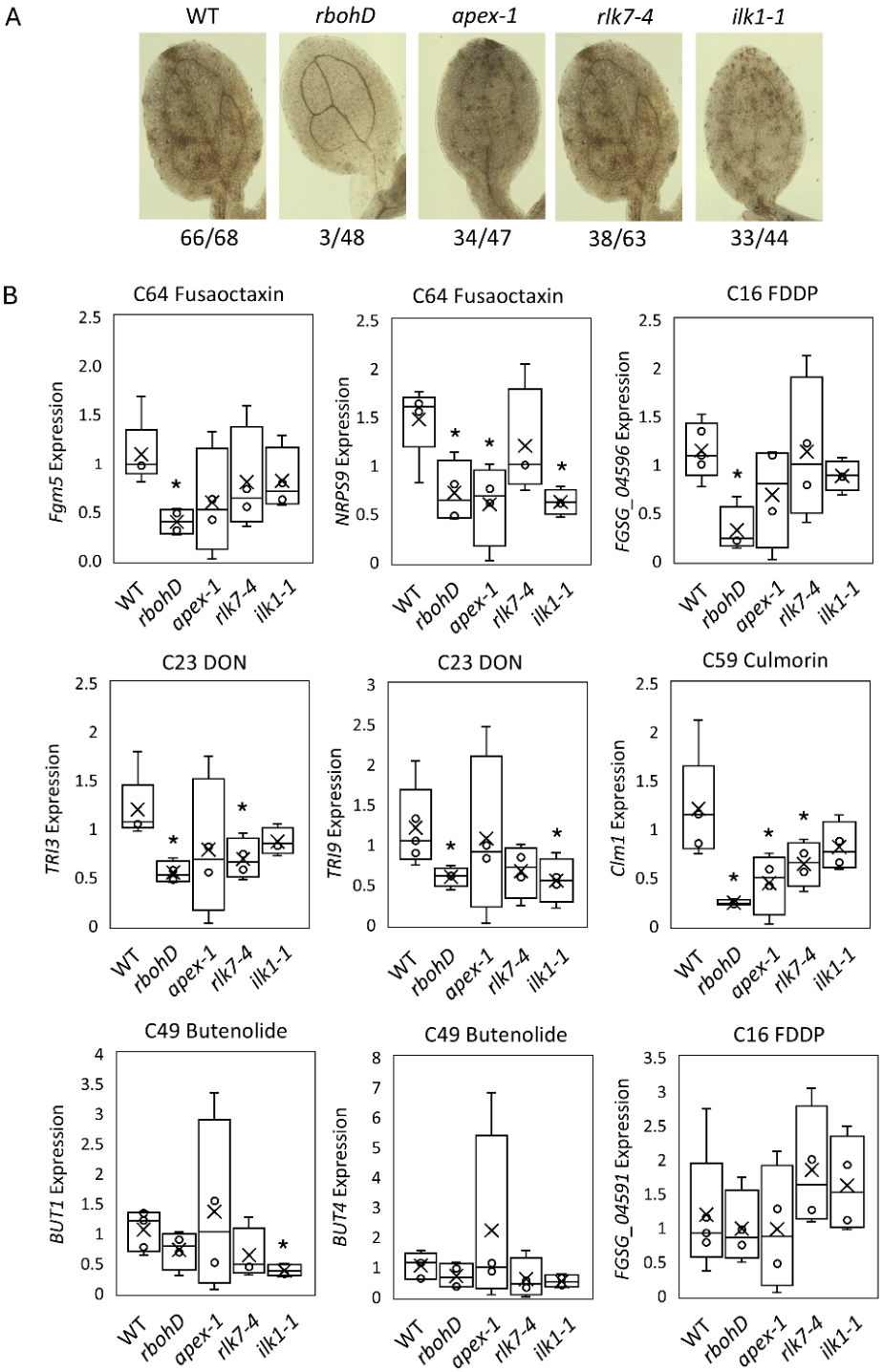

Figure 9. DON and fusaoctaxin biosynthetic gene expression are induced by specific plant susceptibility genes and H_2O_2. A) Visualization of H_2O_2 accumulation in Arabidopsis WT Col-0 and Arabidopsis mutants (*rbohD, apex-1, rlk7-4* & *ilk1-1*) cotyledons. Seedlings were inoculated

with *F. graminearum* DAOM233423 strain and harvested at 3 dpi. ROS was visualized by DAB staining for H_2O_2. The numbers under each image indicate total of H_2O_2 observed out of total seedlings. H_2O_2 accumulation capture with Zeiss Axio Imager M2 compound. The experiment was repeated three times with similar results. B) The box plots represent the ratio of fungal gene expression relative to fungal housekeeping genes (*GAPDH, Fg β-tubulin*). Arabidopsis WT Col-0 and Arabidopsis mutants (*rbohD, apex-1, rlk7-4 & ilk1-1*). Seedlings were infected with *F. graminearum* DAOM233423 strain and harvested at 3 dpi (n=6). An asterisk (*) indicates a statistically significant difference determined by one-tailed t-test ($p<0.05$). The experiment was repeated three times. The data from one experiment is plotted here.

4. Discussion

In this study, we showed that *F. graminearum* secondary metabolite biosynthesis genes and CAZyme genes are induced during Arabidopsis seedling infection and that specific secondary metabolites contribute to virulence. A single host gene could influence the fungal regulation of virulence-promoting secondary metabolite gene expression suggesting that regulating mycotoxin production during infection may be possible through genetic manipulation of the host. We confirmed that the host *RbohD* regulated both ROS production and expression of the DON, FDDP and fusaoctaxin virulence factors in Arabidopsis and that these virulence factors influenced callose accumulation in the host.

4.1 *In planta* expressed BGCs are *RbohD*-dependent

A subset of *F. graminearum* BGCs are consistently expressed within different plant hosts and tissue types suggesting their involvement in pathogenesis. Harris et al. profiled *F. graminearum* gene expression during infection of wheat, barley and maize floral tissues showing that DON, butenolide, fusaoctaxin, gramillin and culmorin BGCs were expressed in multiple hosts (Harris et al. 2016). Additionally, a meta-analysis of *in planta* expressed genes across studies in barley, wheat or *in vitro* revealed that the trichothecene, gramillin, butenolide, fusaoctaxin and culmorin BGCs were consistently expressed *in planta* (Sieber et al. 2014). Interestingly, we identified some of these clusters as *RbohD*-dependent in our study. It remains unclear if the impact of *RbohD* on fungal gene expression is a direct or indirect effector or if it dependent on the ROS-producing influence of the gene. Here, we showed that a *RbohD*-dependent H_2O_2 burst occurs at 3 dpi with *F. graminearum*, consistent with the established role of RBOHD as a major source of stress-induced ROS bursts during *Pseudomonas syringae* pv. *tomato* infection (Torres et al. 2005; Morales et al. 2016). *RbohD* also promotes susceptibility in the Arabidopsis–*Alternaria brassicicola* interaction it influences cell death and pathogen spread (Pogány et al. 2009; Macioszeket al. 2024). Importantly, the reduced H_2O_2 signal in *rbohD* mutant was not associated with impaired infection, as trypan blue staining revealed fungal hyphae and cell death, consistent with fungal colonization in *rbohD* seedlings. These findings suggest that any resistance phenotype in *rbohD* mutant is unlikely to result from blocked pathogen entry, since fungal hyphae are still observed in *rbohD* mutant tissues by trypan blue staining. Indeed, previous work indicates increased callose deposition during *F. graminearum* infection in *rbohD* suggesting penetration is still occurring and host defense responses are higher than in the WT plants (Brauer et al. 2024).

Consistent with this idea, several infection-associated BGCs show reduced transcript accumulation in the *rbohD* mutant background, indicating that fungal secondary metabolite expression is host-genotype dependent. Thus, the host environment seems to be shaped by *RbohD* expression to influence fungal signalling and make the host more susceptible to infection. This would be in line with type III FHB resistance where some genotypes have less DON accumulation, potentially due to the impact of fungal transcriptional reprogramming. Evidence from additional studies supports a functional link between host redox status and *F. graminearum* BGC transcriptional regulation. DON treatment in wheat rapidly induces H_2O_2 accumulation and defence responses (Desmond et al. 2008). In addition, early FHB responses in wheat include induction of antioxidant enzymes which differs between resistant and susceptible genotypes (Spanic et al. 2017). Finally, exogenous H_2O_2 alters *TRI* gene expression in vitro, supporting the idea that ROS-related cues can modulate DON-pathway regulation (Ponts et al. 2007). The *Fgap1* gene encodes an oxidative stress-responsive bZIP transcription factor required for oxidative stress-dependent changes in trichothecene accumulation and *TRI* transcript levels (Montibus et al. 2013). In addition, fungal stress-signalling pathways that respond to oxidative stress also intersect with virulence and DON output, as the Hog1 MAPK pathway contributes to oxidative stress tolerance, plant infection, and full DON production (Zheng et al. 2012). Finally, the DON regulator TRI6 can control additional BGCs beyond the *TRI* cluster, providing a plausible route by which an ROS-linked DON regulatory program could coordinate induction of other infection-associated clusters we observe as *RbohD*-enriched such as C16, C49 and C64 (Nasmith et al. 2011; Sieber et al. 2014; Shostak et al. 2020). Together, these results support a model that RBOHD host ROS signalling acts as an upstream cue that coordinates multiple *F. graminearum* secondary metabolite programs

during early infection, rather than BGC induction being driven solely by an intrinsic fungal timetable.

While RBOHD-derived ROS is an important cue for plant cellular signalling, the *RbohD* gene has pleiotropic effects on plant physiology and thus it is important to consider other potential cues that may influence *F. graminearum* expression. In infections with the *Pseudomonas syringae* pv. *tomato* bacteria, Chaouch et al. (2012) propose that recognition of the avirulent bacterium triggers an apoplastic ROS burst that increases intracellular ROS and SA, alongside feedback regulation that would otherwise dampen RBOHD activity. In this model, SA counteracts oxidative-stress driven repression of *RbohD*, helping prevent premature arrest of the signalling cascade and enabling cell-to-cell signalling. Importantly, despite similar SA kinetics in *rbohD* and WT during the incompatible interaction, loss of *RbohD* caused a strong, selective increase in the phytoalexin-like defence metabolite scopoletin (nearly 16-fold higher) (Chaouch et al. 2012). Moreover, non-targeted profiling showed that *rbohD* and *rbohF* strongly affected metabolite profiles over time in response to both avirulent and virulent bacterial strains, supporting the broader conclusion that ROS signalling can reshape infection-associated chemistry (Chaouch et al. 2012). Together, these studies support the idea that *RBOHD* shapes the *in planta* environment beyond ROS alone, which raises the possibility that other susceptibility genes may also change the host cues the fungus encounters during infection.

4.3 Additional susceptibility pathways beyond H_2O_2

Although *rbohD* had the strongest effect on fungal secondary metabolite expression, additional resistant mutants showed minor effects on the expression of fungal BGCs with no

impact on ROS, suggesting that different immune mechanism contribute to host susceptibility. *ILK1, RLK7*, and *APEX1* mutations did not strongly alter ROS accumulation, yet the expression of several fungal BGCs were still affected, indicating that not all fungal virulence programs depend primarily on ROS (Pitorre et al. 2010; Smakowska-Luzan et al. 2018; Manes et al. 2021). A previous study showed that ILK1 limits *Pseudomonas syringae* pv. *tomato* growth through its kinase activity, likely through regulation of potassium uptake and the HAK5 transporter (Brauer et al. 2016). During infection, the authors report that gramillin suppresses callose deposition, promotes *NRPS9* expression and that *ilk1-1* mutant displays increased callose deposits in infected seedlings (Brauer et al. 2024). In addition, gramillin elicits a rapid ROS burst that requires *ILK1* and *RBOHD*, linking ionophore-triggered responses and regulation of *F. graminearum* secondary metabolite production (Brauer et al. 2024). *RLK7* is a leucine-rich repeat receptor-like kinase (LRR-RLK) with an extracellular LRR ectodomain, a single transmembrane region, and a cytosolic kinase domain, and it has been implicated in both stress responses and immunity (Chowdhury and Mubassir 2022). Researchers also describe *RLK7* as a receptor that recognizes the PIP peptides which are DAMPs and contribute to responses against both bacterial and fungal challenges (Chowdhury and Mubassir 2022). In the Arabidopsis-*F. graminearum* seedling assay, *rlk7* mutant showed enhanced resistance, consistent with *RLK7* acting as a susceptibility factor during Arabidopsis-*F. graminearum* infection (Manes et al. 2021). Interestingly, the same study found that RLK7 is still required for some chitin-triggered immune outputs in mature leaves, as chitin-induced callose deposition was decreased in *rlk7* mutant relative to WT plants (Manes et al. 2021). APEX is a leucine-rich repeat receptor-like kinase (LRR-RLK), its thought to function as a co-receptor (Smkowska-Luzan et al., 2018). In the *Arabidopsis-F. graminearum* pathosystem, the *apex* mutant was more resistant relative to the WT (Manes et al. 2021). During *F. graminearum*

infection, *apex* seedlings accumulate SA at levels similar to WT at 3 dpi, suggesting the resistance phenotype is not simply explained by higher SA (Manes et al. 2021). APEX prevents formation of the *FLS2-BAK1* complex and suppresses *FLS2* signalling (Smakowska-Luzan et al. 2018). Consistent with flg22 perception normally promoting FLS2–BAK1 complex formation to initiate immune signalling, *apex* mutants show stronger flg22-triggered outputs, including increased *FLS2-BAK*1 complex formation, MAPK activation, and *FRK1* induction, along with an enhanced flg22-induced ROS burst (Sun et al. 2013; Manes et al. 2021). Overall, these susceptibility genes likely promote infection through different host processes compared with *RbohD.*

4.4 Callose suppression as a conserved virulence strategy

F. graminearum actively suppresses host defensive barrier formation and several virulence factors target callose production to promote fungal invasion and spread. Consistent with previous work, DON production contributes to disease in wheat, barley, and maize, and our results extend this importance to Arabidopsis seedlings (Jansen et al. 2005; Maier et al. 2006; Harris et al. 2007). In addition, fusaoctaxin and FDDP have been implicated in promoting virulence in cereals, and our results support a role in promoting Arabidopsis infection as well (Jia et al. 2019; Westphal et al. 2019; Hicks et al. 2023). In our assay, *F. poae* and *F. sporotrichioides* were less virulent than *F. graminearum*, consistent with different *Fusarium* species deploying distinct virulence toolkits. *F. sporotrichioides* is typically associated with type A trichothecenes (T-2 toxin) rather than DON (Brown et al. 2001; Busman et al. 2011). By contrast, *F. poae* is often reported as a less aggressive FHB-associated species, it is commonly linked to nivalenol, fusarenon-X and other metabolites such as enniatins and beauvericin (Kulik and Jestoi 2009; Pasquali et al. 2016; Nazari et al. 2019; Tan et al. 2021). To test whether these secondary metabolites influence host barrier defences, we

quantified callose deposits following infection with each mutant and found that *Δtri5, Δfgm5* and *ΔC16* induced higher callose deposition than WT *F. graminearum*. Notably, in wheat coleoptiles, a fusaoctaxin-cluster mutant elicits stronger callose deposition at hyphal fronts than WT (Jia et al. 2019; Westphal et al. 2019; Tang et al. 2021). This callose-targeting mechanism appears to extend to DON as well. A study in wheat provides evidence that DON promotes cell-to-cell invasion by facilitating traversal through plasmodesmata, consistent with disruption of defensive barriers, where callose deposition serves as a central component (Blümke et al. 2014; Armer et al. 2024). More broadly, *F. graminearum* virulence factors can suppress callose formation during wheat head infection where a secreted lipase FGL1 inhibits callose formation to promote spread in wheat spikes (Blümke et al. 2014; Ellinger et al. 2014). Together, the increased callose with *Δtri5, Δfgm5* and *ΔC16* and their reduced abundance suggest these metabolites may promote colonization in part by counteracting host cell-wall barrier responses, directly or indirectly. Since these virulence factors function in both cereals and Arabidopsis, our findings suggest that *RbohD*-dependent host cues help tune a conserved *F. graminearum* virulence program rather than driving an Arabidopsis-specific transcriptional response. Together, these results suggest that the infection strategies and transcriptional regulation used by *F. graminearum* in Arabidopsis seedlings are at least partly analogous to those observed in cereal crops.

Overall, this study shows that *F. graminearum* deploys at least a partially overlapping induction of BGCs during both Arabidopsis seedling infection and cereal infection. Three known or suspected virulence factors including DON, fusaoctaxin, and FDDP in cereals also had a virulence function in Arabidopsis seedlings and suppressed callose production. Taken together, this supports the use of Arabidopsis seedling infection in capturing *F. graminearum* infection

biology, while providing a tractable system to dissect how host cues (ROS-dependent and ROS-independent) shape fungal secondary metabolite deployment during disease progression.

5. Conclusion & Future directions

This thesis shows that *F. graminearum* deploys the same secondary metabolite virulence factors during Arabidopsis seedling infection as it uses to infect cereals. Induction seems to be dependent on the *RbohD* host gene suggesting a connection with the host redox state. Together, these findings position host signals as shaping fungal transcriptional programs during infection, and they provide a framework for understanding how host immune outputs can also function as cues that promote fungal pathogenicity.

Taken together with prior work, these results also highlight important unresolved questions about how host genotype and physiology regulate fungal expression of secondary metabolite biosynthetic genes. We hypothesize that fungal secondary metabolite production is influenced by host-derived ROS, either because WT plants provide a redox-dependent signal that is reduced in mutant backgrounds, or because certain mutant contexts generate conditions that suppress fungal activation. By linking Arabidopsis *RbohD*-dependent host responses to induction of *F. graminearum* secondary metabolite clusters, this study clarifies how host factors can shape fungal pathogenicity programs. Importantly, although Arabidopsis is not a natural cereal host, it provides a genetically tractable platform to identify conserved host cues and fungal regulatory nodes that can be tested directly in crops. Because DON and other secondary metabolites underpin FHB severity and mycotoxin contamination in cereals, identifying the fungal sensors and transcriptional regulators that respond to ROS-shaped host environments could inform strategies to uncouple

fungal development from host cues, ultimately reducing both disease and toxin accumulation in crop systems.

Future work should focus on establishing whether RBOHD-derived ROS is a direct regulator of fungal secondary metabolite induction and timing. A key next step is to manipulate redox conditions during infection by applying exogenous H_2O_2 and using ROS-scavenging approaches in parallel, then testing whether secondary metabolite pathway transcripts are induced or shifted in timing, particularly in *rbohD* mutant background. In parallel, targeted metabolite measurements across time points and host genotypes will be essential to link transcriptional induction to chemical output and to prioritize the most biologically relevant metabolites during infection. Identifying the fungal sensing and regulatory nodes that connect oxidative or ROS-shaped host environments to activation of specific pathways such as redox-responsive transcription factors, stress-activated signalling modules, or global secondary metabolite regulators will clarify how the fungus interprets host cues and may reveal intervention points. Because *RbohD* reshapes host physiology beyond ROS itself, additional work should integrate other *RbohD*-linked host outputs (callose deposition and cell wall reinforcement) to determine which host changes best predict fungal metabolite responses. Finally, translating key observations to cereal-relevant tissues will strengthen agricultural significance by testing whether altering host redox dynamics in wheat or barley shifts fungal secondary metabolite expression and DON accumulation during FHB. Thus, these directions will move the model from association to help define strategies to reduce fungal virulence and mycotoxin risk.

In addition, the observation that *F. poae* and *F. sporotrichioides* produce slower symptom development and lower *in planta* fungal abundance than *F. graminearum* highlights an opportunity to use the Arabidopsis seedling system for controlled, cross-species comparisons of virulence.

Future work could determine whether these differences reflect delayed infection versus fundamentally different infection programs by comparing species at matched infection stage such as sampling when each reaches similar fungal/plant ratios rather than matched dpi. Combining stage-matched sampling with microscopy-based quantification of early infection events (penetration frequency, hyphal expansion, and tissue spread) would help localize where the species diverge during infection. Parallel profiling of virulence-associated modules such as CAZyme suites, secondary metabolite genes, and stress-response genes, alongside targeted metabolite measurements normalized to fungal burden, would clarify whether reduced disease reflects stronger host restriction, reduced deployment of fungal virulence outputs, or lower tolerance to host-associated stresses.

Beyond advancing our understanding of host-pathogen signalling, these findings also have broader societal relevance. FHB reduces cereal yield and grain quality while increasing the risk of DON contamination, affecting food and feed safety and contributing to economic losses across the supply chain. By identifying host immune outputs particularly *RbohD*-linked redox dynamics as cues that shape *F. graminearum* secondary metabolite programs, this thesis contributes to a more mechanistic understanding of how toxin-associated virulence is triggered *in planta*. This matters beyond basic biology, as interventions that disrupt cue-dependent activation such as breeding for host traits that limit pathogen-favorable redox environments, or targeting fungal regulators that translate oxidative cues into DON induction could reduce both disease severity and mycotoxin accumulation. Ultimately, improving our ability to anticipate and mitigate toxin production supports more reliable cereal production, safer food and livestock feed, and reduced losses associated with rejected or downgraded grain, thereby strengthening food security and producer livelihoods.

6. References

Adpressa, Donovon A., Lanelle R. Connolly, Zachary M. Konkel, George F. Neuhaus, Xiao L. Chang, Brett R. Pierce, Kristina M. Smith, Michael Freitag, and Sandra Loesgen. "A metabolomics-guided approach to discover *Fusarium graminearum* metabolites after removal of a repressive histone modification." *Fungal Genetics and Biology* 132 (2019): 103256.

Agrios, George N. *Plant pathology*. Elsevier, 2005.

Alexander, Nancy J., Susan P. McCormick, Cees Waalwijk, Theo van der Lee, and Robert H. Proctor. "The genetic basis for 3-ADON and 15-ADON trichothecene chemotypes in Fusarium." *Fungal Genetics and Biology* 48, no. 5 (2011): 485-495.

Alisaac, Elias, and Anne-Katrin Mahlein. "Fusarium head blight on wheat: Biology, modern detection and diagnosis and integrated disease management." *Toxins* 15, no. 3 (2023): 192.

Alouane, Tarek, Hélène Rimbert, Jörg Bormann, Gisela A. González-Montiel, Sandra Loesgen, Wilhelm Schäfer, Michael Freitag, Thierry Langin, and Ludovic Bonhomme. "Comparative genomics of eight *Fusarium graminearum* strains with contrasting aggressiveness reveals an expanded open pangenome and extended effector content signatures." *International journal of molecular sciences* 22, no. 12 (2021): 6257.

Armer, Victoria J., Martin Urban, Tom Ashfield, Michael J. Deeks, and Kim E. Hammond-Kosack. "The trichothecene mycotoxin deoxynivalenol facilitates cell-to-cell invasion during wheat-tissue colonization by *Fusarium graminearum*." *Molecular plant pathology* 25, no. 6 (2024): e13485.

Bahadoor, Adilah, Elizabeth K. Brauer, Whynn Bosnich, Danielle Schneiderman, Anne Johnston, Yves Aubin, Barbara Blackwell, Jeremy E. Melanson, and Linda J. Harris. "Gramillin A and B: Cyclic lipopeptides identified as the nonribosomal biosynthetic products of *Fusarium graminearum*." *Journal of the American Chemical Society* 140, no. 48 (2018): 16783-16791.

Bai, Guihua, Zhenqi Su, and Jin Cai. "Wheat resistance to Fusarium head blight." *Canadian Journal of Plant Pathology*40, no. 3 (2018): 336-346.

Basenko, Evelina Y., Jane A. Pulman, Achchuthan Shanmugasundram, Omar S. Harb, Kathryn Crouch, David Starns, Susanne Warrenfeltz et al. "FungiDB: an integrated bioinformatic resource for fungi and oomycetes." *Journal of Fungi* 4, no. 1 (2018): 39.

Bian, Guangkai, Anwei Hou, Yujie Yuan, Ben Hu, Shu Cheng, Ziling Ye, Yingtong Di, Zixin Deng, and Tiangang Liu. "Metabolic engineering-based rapid characterization of a

sesquiterpene cyclase and the skeletons of fusariumdiene and fusagramineol from *Fusarium graminearum*." *Organic letters*20, no. 6 (2018): 1626-1629.

Bills, Gerald F., and James B. Gloer. "Biologically active secondary metabolites from the fungi." *Microbiology spectrum*4, no. 6 (2016): 10-1128.

Blümke, Antje, Christian Falter, Cornelia Herrfurth, Björn Sode, Rainer Bode, Wilhelm Schäfer, Ivo Feussner, and Christian A. Voigt. "Secreted fungal effector lipase releases free fatty acids to inhibit innate immunity-related callose formation during wheat head infection." *Plant physiology* 165, no. 1 (2014): 346-358.

Boedi, Stefan, Harald Berger, Christian Sieber, Martin Münsterkötter, Imer Maloku, Benedikt Warth, Michael Sulyok et al. "Comparison of *Fusarium graminearum* transcriptomes on living or dead wheat differentiates substrate-responsive and defense-responsive genes." *Frontiers in Microbiology* 7 (2016): 1113.

Brakhage, Axel A. "Regulation of fungal secondary metabolism." *Nature Reviews Microbiology* 11, no. 1 (2013): 21-32.

Brauer, Elizabeth K., Nagib Ahsan, Renee Dale, Naohiro Kato, Alison E. Coluccio, Miguel A. Piñeros, Leon V. Kochian, Jay J. Thelen, and Sorina C. Popescu. "The Raf-like kinase ILK1 and the high affinity K+ transporter HAK5 are required for innate immunity and abiotic stress response." *Plant physiology* 171, no. 2 (2016): 1470-1484.

Brauer, Elizabeth K., Rajagopal Subramaniam, and Linda J. Harris. "Regulation and dynamics of gene expression during the life cycle of *Fusarium graminearum*." *Phytopathology* 110, no. 8 (2020): 1368-1374.

Brauer, Elizabeth K., Nagib Ahsan, George V. Popescu, Jay J. Thelen, and Sorina C. Popescu. "Back from the dead: the atypical kinase activity of a pseudokinase regulator of cation fluxes during inducible immunity." Frontiers in plant science 13 (2022): 931324.

Brauer, Elizabeth K., Whynn Bosnich, Kirsten Holy, Indira Thapa, Srinivasan Krishnan, Moatter Syed, Melissa Bredow et al. "A cyclic lipopeptide from *Fusarium graminearum* targets plant membranes to promote virulence." *Cell Reports* 43, no. 7 (2024).

Brown, Daren W., Susan P. McCormick, Nancy J. Alexander, Robert H. Proctor, and Anne E. Desjardins. "A genetic and biochemical approach to study trichothecene diversity in *Fusarium sporotrichioides* and *Fusarium graminearum*." *Fungal Genetics and Biology* 32, no. 2 (2001): 121-133.

Brown, Daren W., Susan P. McCormick, Nancy J. Alexander, Robert H. Proctor, and Anne E. Desjardins. "Inactivation of a cytochrome P-450 is a determinant of trichothecene diversity in *Fusarium* species." *Fungal Genetics and Biology* 36, no. 3 (2002): 224-233.

Buerstmayr, Maria, Barbara Steiner, and Hermann Buerstmayr. "Breeding for Fusarium head blight resistance in wheat—Progress and challenges." Plant breeding 139, no. 3 (2020): 429-454.

Buerstmayr, Maria, Christian Wagner, Tetyana Nosenko, Jimmy Omony, Barbara Steiner, Thomas Nussbaumer, Klaus FX Mayer, and Hermann Buerstmayr. "Fusarium head blight resistance in European winter wheat: insights from genome-wide transcriptome analysis." *BMC genomics* 22, no. 1 (2021): 470.

Busman, Mark, Stephen M. Poling, and Chris M. Maragos. "Observation of T-2 toxin and HT-2 toxin glucosides from *Fusarium sporotrichioides* by liquid chromatography coupled to tandem mass spectrometry (LC-MS/MS)." *Toxins* 3, no. 12 (2011): 1554-1568.

Chaouch, Sejir, Guillaume Queval, and Graham Noctor. "AtRbohF is a crucial modulator of defence-associated metabolism and a key actor in the interplay between intracellular oxidative stress and pathogenesis responses in Arabidopsis." *The Plant Journal* 69, no. 4 (2012): 613-627.

Chen, Yun, H. Corby Kistler, and Zhonghua Ma. "*Fusarium graminearum* trichothecene mycotoxins: biosynthesis, regulation, and management." Annual review of phytopathology 57, no. 1 (2019): 15-39.

Choquer, Mathias, Christine Rascle, Isabelle R. Gonçalves, Amélie de Vallée, Cécile Ribot, Elise Loisel, Pavlé Smilevski et al. "The infection cushion: a fungal “weapon” of plant-biomass destruction." *bioRxiv* (2020): 2020-06.

Choquer, Mathias, Christine Rascle, Isabelle R. Gonçalves, Amélie de Vallée, Cécile Ribot, Elise Loisel, Pavlé Smilevski et al. "The infection cushion: a fungal “weapon” of plant-biomass destruction." *bioRxiv* (2020): 2020-06.

Chowdhury, Ramen, and M. H. M. Mubassir. "How Arabidopsis Receptor-Like Kinase 7 (RLK7) Manifests: Delineating Its Structure and Function." *Advances in Agriculture* 2022, no. 1 (2022): 4715110.

Connolly, Lanelle R., Kristina M. Smith, and Michael Freitag. "The *Fusarium graminearum* histone H3 K27 methyltransferase KMT6 regulates development and expression of secondary metabolite gene clusters." *PLoS genetics* 9, no. 10 (2013): e1003916.

Cuzick, Alayne, Martin Urban, and Kim Hammond-Kosack. "*Fusarium graminearum* gene deletion mutants map1 and tri5 reveal similarities and differences in the pathogenicity requirements to cause disease on Arabidopsis and wheat floral tissue." *New Phytologist* 177, no. 4 (2008): 990-1000.

Daudi, Arsalan, and Jose A. O’brien. "Detection of hydrogen peroxide by DAB staining in Arabidopsis leaves." *Bio-protocol*2, no. 18 (2012): e263-e263.

Daudi, Arsalan, Zhenyu Cheng, Jose A. O'Brien, Nicole Mammarella, Safina Khan, Frederick M. Ausubel, and G. Paul Bolwell. "The apoplastic oxidative burst peroxidase in Arabidopsis is a major component of pattern-triggered immunity." *The Plant Cell* 24, no. 1 (2012): 275-287.

Deng, Ying, Li You, Xu Wang, Wenda Wu, Kamil Kuca, Qinghua Wu, and Wei Wei. "Deoxynivalenol: emerging toxic mechanisms and control strategies, current and future perspectives." *Journal of agricultural and food chemistry* 71, no. 29 (2023): 10901-10915.

Desjardins, Anne E. *Fusarium mycotoxins: chemistry, genetics, and biology*. 2006.

Desmond, Olivia J., John M. Manners, Amber E. Stephens, Donald J. Maclean, Peer M. Schenk, Donald M. Gardiner, Alan L. Munn, and Kemal Kazan. "The *Fusarium* mycotoxin deoxynivalenol elicits hydrogen peroxide production, programmed cell death and defence responses in wheat." *Molecular plant pathology* 9, no. 4 (2008): 435-445.

De Silva, N. I. "Mycosphere essays 9: defining biotrophs and hemibiotrophs." *Mycosphere* 7, no. 5 (2016): 545-559.

Dobin, Alexander, Carrie A. Davis, Felix Schlesinger, Jorg Drenkow, Chris Zaleski, Sonali Jha, Philippe Batut, Mark Chaisson, and Thomas R. Gingeras. "STAR: ultrafast universal RNA-seq aligner." *Bioinformatics* 29, no. 1 (2013): 15-21.

Dodds, Peter N., and John P. Rathjen. "Plant immunity: towards an integrated view of plant–pathogen interactions." *Nature Reviews Genetics* 11, no. 8 (2010): 539-548.

Eagan, Justin L., and Nancy P. Keller. "Fungal secondary metabolism." *Current Biology* 35, no. 11 (2025): R503-R508.

Ekwomadu, Theodora I., Stephen A. Akinola, and Mulunda Mwanza. "*Fusarium* mycotoxins, their metabolites (free, emerging, and masked), food safety concerns, and health impacts." *International Journal of Environmental Research and Public Health* 18, no. 22 (2021): 11741.

Ellinger, Dorothea, Björn Sode, Christian Falter, and Christian A. Voigt. "Resistance of callose synthase activity to free fatty acid inhibition as an indicator of Fusarium head blight resistance in wheat." *Plant signalling & behavior* 9, no. 7 (2014): e28982.

Evans, Matthew J., Won-Gyu Choi, Simon Gilroy, and Richard J. Morris. "A ROS-assisted calcium wave dependent on the AtRBOHD NADPH oxidase and TPC1 cation channel propagates the systemic response to salt stress." *Plant Physiology* 171, no. 3 (2016): 1771-1784.

Fedoreyeva, Larisa Ivanovna. "ROS as signalling molecules to initiate the process of plant acclimatization to abiotic stress." *International Journal of Molecular Sciences* 25, no. 21 (2024): 11820.

Ferrari, Simone, Luca Sella, M. Janni, Giulia De Lorenzo, Francesco Favaron, and R. D'ovidio. "Transgenic expression of polygalacturonase-inhibiting proteins in Arabidopsis and wheat increases resistance to the flower pathogen *Fusarium graminearum*." *Plant Biology* 14 (2012): 31-38.

Frandsen, Rasmus JN, Nikoline J. Nielsen, Nicolai Maolanon, Jens C. Sørensen, Stefan Olsson, John Nielsen, and Henriette Giese. "The biosynthetic pathway for aurofusarin in *Fusarium graminearum* reveals a close link between the naphthoquinones and naphthopyrones." *Molecular microbiology* 61, no. 4 (2006): 1069-1080.

Gaffoor, Iffa, Daren W. Brown, Ron Plattner, Robert H. Proctor, Weihong Qi, and Frances Trail. "Functional analysis of the polyketide synthase genes in the filamentous fungus Gibberella zeae (anamorph *Fusarium graminearum*)." *Eukaryotic Cell* 4, no. 11 (2005): 1926-1933.

Galletti, Roberta, Carine Denoux, Stefano Gambetta, Julia Dewdney, Frederick M. Ausubel, Giulia De Lorenzo, and Simone Ferrari. "The AtrbohD-mediated oxidative burst elicited by oligogalacturonides in Arabidopsis is dispensable for the activation of defense responses effective against *Botrytis cinerea*." *Plant physiology* 148, no. 3 (2008): 1695-1706.

Gardiner, Donald M., Kemal Kazan, and John M. Manners. "Nutrient profiling reveals potent inducers of trichothecene biosynthesis in *Fusarium graminearum*." *Fungal genetics and biology* 46, no. 8 (2009): 604-613.

Gilroy, Simon, Maciej Białasek, Nobuhiro Suzuki, Magdalena Górecka, Amith R. Devireddy, Stanisław Karpiński, and Ron Mittler. "ROS, calcium, and electric signals: key mediators of rapid systemic signalling in plants." *Plant physiology* 171, no. 3 (2016): 1606-1615.

Goswami, Rubella S., and H. Corby Kistler. "Heading for disaster: *Fusarium graminearum* on cereal crops." *Molecular plant pathology* 5, no. 6 (2004): 515-525.

Government of Ontario. n.d. "Fusarium Head Blight." Ontario Crop IPM. Accessed May 1, 2026. https://cropipm.omafra.gov.on.ca/en-ca/crops/wheat/diseases/d262410f-0861-4e9b-9f5e-8dd25e74f321

Gunupuru, L. R., A. Perochon, and F. M. Doohan. "Deoxynivalenol resistance as a component of FHB resistance." *Tropical Plant Pathology* 42, no. 3 (2017): 175-183.

Hao, Guixia, Robert H. Proctor, Daren W. Brown, Nicholas A. Rhoades, Todd A. Naumann, HyeSeon Kim, Santiago Gutièrrez, and Susan P. McCormick. "TRI14 is critical for

Fusarium graminearum infection and spread in wheat." *Applied Microbiology* 4, no. 2 (2024): 839-855.

Harris, L. J., Ac E. Desjardins, R. D. Plattner, P. Nicholson, G. Butler, J. C. Young, G. Weston, R. H. Proctor, and T. M. Hohn. "Possible role of trichothecene mycotoxins in virulence of *Fusarium graminearum* on maize." *Plant Disease* 83, no. 10 (1999): 954-960.

Harris, L. J., N. J. Alexander, A. Saparno, B. Blackwell, S. P. McCormick, A. E. Desjardins, L. S. Robert et al. "A novel gene cluster in *Fusarium graminearum* contains a gene that contributes to butenolide synthesis." *Fungal Genetics and Biology* 44, no. 4 (2007): 293-306.

Harris, Linda J., Margaret Balcerzak, Anne Johnston, Danielle Schneiderman, and Thérèse Ouellet. "Host-preferential *Fusarium graminearum* gene expression during infection of wheat, barley, and maize." *Fungal Biology* 120, no. 1 (2016): 111-123.

Hicks, Carmen, Thomas E. Witte, Amanda Sproule, Anne Hermans, Samuel W. Shields, Ronan Colquhoun, Chris Blackman, Christopher N. Boddy, Rajagopal Subramaniam, and David P. Overy. "CRISPR-Cas9 gene editing and secondary metabolite screening confirm *Fusarium graminearum* C16 biosynthetic gene cluster products as decalin-containing diterpenoid pyrones." *Journal of Fungi* 9, no. 7 (2023): 695.

Hoogendoorn, Koen, Lena Barra, Cees Waalwijk, Jeroen S. Dickschat, Theo AJ Van der Lee, and Marnix H. Medema. "Evolution and diversity of biosynthetic gene clusters in Fusarium." *Frontiers in microbiology* 9 (2018): 1158.

Hou, Rui, Cong Jiang, Qian Zheng, Chenfang Wang, and Jin-Rong Xu. "The AreA transcription factor mediates the regulation of deoxynivalenol (DON) synthesis by ammonium and cyclic adenosine monophosphate (cAMP) signalling in F usarium graminearum." *Molecular plant pathology* 16, no. 9 (2015): 987-999.

Ireta, M. J., Jal Tepatitlan, and L. Gilchrist. *Fusarium head scab of wheat (Fusarium graminearum Schwabe)*. No. 21a. 1994.

Jansen, Carin, Diter Von Wettstein, Wilhelm Schäfer, Karl-Heinz Kogel, Angelika Felk, and Frank J. Maier. "Infection patterns in barley and wheat spikes inoculated with wild-type and trichodiene synthase gene disrupted *Fusarium graminearum*." *Proceedings of the National Academy of Sciences* 102, no. 46 (2005): 16892-16897.

Jia, Lei-Jie, Hao-Yu Tang, Wan-Qiu Wang, Ting-Lu Yuan, Wan-Qian Wei, Bo Pang, Xue-Min Gong et al. "A linear nonribosomal octapeptide from *Fusarium graminearum* facilitates cell-to-cell invasion of wheat." *Nature communications* 10, no. 1 (2019): 922.

Jiang, Cong, Chengkang Zhang, Chunlan Wu, Panpan Sun, Rui Hou, Huiquan Liu, Chenfang Wang, and Jin-Rong Xu. "TRI6 and TRI10 play different roles in the regulation of

deoxynivalenol (DON) production by cAMP signalling in *Fusarium graminearum*." *Environmental Microbiology* 18, no. 11 (2016): 3689-3701.

Jin, Jian-Ming, Jungkwan Lee, and Yin-Won Lee. "Characterization of carotenoid biosynthetic genes in the ascomycete Gibberella zeae." *FEMS microbiology letters* 302, no. 2 (2010): 197-202.

Jørgensen, Simon Hartung, Rasmus John Norman Frandsen, Kristian Fog Nielsen, Erik Lysøe, Teis Esben Sondergaard, Reinhard Wimmer, Henriette Giese, and Jens Laurids Sørensen. "*Fusarium graminearum* PKS14 is involved in orsellinic acid and orcinol synthesis." *Fungal Genetics and Biology* 70 (2014): 24-31.

Kadota, Yasuhiro, Ken Shirasu, and Cyril Zipfel. "Regulation of the NADPH oxidase RBOHD during plant immunity." *Plant and Cell Physiology* 56, no. 8 (2015): 1472-1480.

Kazan, Kemal, Donald M. Gardiner, and John M. Manners. "On the trail of a cereal killer: recent advances in *Fusarium graminearum* pathogenomics and host resistance." *Molecular plant pathology* 13, no. 4 (2012): 399-413.

Keller, Melissa D., Gary C. Bergstrom, and Elson J. Shields. "The aerobiology of *Fusarium graminearum*." *Aerobiologia* 30, no. 2 (2014): 123-136.

Kim, Hee-Kyoung, Seunghoon Lee, Seong-Mi Jo, Susan P. McCormick, Robert AE Butchko, Robert H. Proctor, and Sung-Hwan Yun. "Functional roles of FgLaeA in controlling secondary metabolism, sexual development, and virulence in *Fusarium graminearum*." *PLoS One* 8, no. 7 (2013): e68441.

Keller, Nancy P., Geoffrey Turner, and Joan W. Bennett. "Fungal secondary metabolism—from biochemistry to genomics." *Nature reviews microbiology* 3, no. 12 (2005): 937-947.

Keller, Nancy P. "Fungal secondary metabolism: regulation, function and drug discovery." *Nature Reviews Microbiology* 17, no. 3 (2019): 167-180.

Kim, Yong-Tae, Ye-Ryun Lee, Jianming Jin, Kap-Hoon Han, Hun Kim, Jin-Cheol Kim, Theresa Lee, Sung-Hwan Yun, and Yin-Won Lee. "Two different polyketide synthase genes are required for synthesis of zearalenone in Gibberella zeae." *Molecular Microbiology* 58, no. 4 (2005): 1102-1113.

Kolberg, Liis, Uku Raudvere, Ivan Kuzmin, Priit Adler, Jaak Vilo, and Hedi Peterson. "g: Profiler—interoperable web service for functional enrichment analysis and gene identifier mapping (2023 update)." *Nucleic acids research* 51, no. W1 (2023): W207-W212.

Kulik, T., and M. Jestoi. "Quantification of *Fusarium poae* DNA and associated mycotoxins in asymptomatically contaminated wheat." *International Journal of Food Microbiology* 130, no. 3 (2009): 233-237.

Lapin, Dmitry, and Guido Van den Ackerveken. "Susceptibility to plant disease: more than a failure of host immunity." *Trends in plant science* 18, no. 10 (2013): 546-554.

Lemmens, Marc, Uwe Scholz, Franz Berthiller, Chiara Dall'Asta, Andrea Koutnik, Rainer Schuhmacher, Gerhard Adam et al. "The ability to detoxify the mycotoxin deoxynivalenol colocalizes with a major quantitative trait locus for Fusarium head blight resistance in wheat." *Molecular plant-microbe interactions* 18, no. 12 (2005): 1318-1324.

Leplat, Johann, Hanna Friberg, Muhammad Abid, and Christian Steinberg. "Survival of *Fusarium graminearum*, the causal agent of Fusarium head blight. A review." *Agronomy for sustainable development* 33, no. 1 (2013): 97-111.

Leplat, Johann, Cécile Héraud, Elodie Gautheron, Pierre Mangin, Laurent Falchetto, and Christian Steinberg. "Colonization dynamic of various crop residues by *Fusarium graminearum* monitored through real-time PCR measurements." *Journal of applied microbiology* 121, no. 5 (2016): 1394-1405.

Li, Chaoqun, Yonghui Zhang, Huan Wang, Lingfeng Chen, Ju Zhang, Manli Sun, Jin-Rong Xu, and Chenfang Wang. "The PKR regulatory subunit of protein kinase A (PKA) is involved in the regulation of growth, sexual and asexual development, and pathogenesis in *Fusarium graminearum*." *Molecular plant pathology* 19, no. 4 (2018): 909-921.

López-Arellanes, Miguel E., Lizbeth Denisse López-Pacheco, Joel H. Elizondo-Luevano, and Georgia María González-Meza. "Algae and Cyanobacteria Fatty Acids and Bioactive Metabolites: Natural Antifungal Alternative Against Fusarium sp." *Microorganisms* 13, no. 2 (2025): 439.

Macioszek, Violetta Katarzyna, Alicja Piotrowska-Niczyporuk, and Andrzej Kiejstut Kononowicz. "Alternaria brassicicola-induced ROS accumulation during black spot disease differentially affects antioxidant efficiency, phenolic content and susceptibility of Brassica species." *Plant Pathology* 73, no. 6 (2024): 1400-1412.

Maier, Frank J., Thomas Miedaner, Birgit Hadeler, Angelika Felk, Siegfried Salomon, Marc Lemmens, Helmut Kassner, and Wilhelm Schäfer. "Involvement of trichothecenes in fusarioses of wheat, barley and maize evaluated by gene disruption of the trichodiene synthase (Tri5) gene in three field isolates of different chemotype and virulence." *Molecular plant pathology* 7, no. 6 (2006): 449-461.

Malz, Sascha, Morten N. Grell, Charlotte Thrane, Frank J. Maier, Pernille Rosager, Angelika Felk, Klaus S. Albertsen et al. "Identification of a gene cluster responsible for the biosynthesis of aurofusarin in the *Fusarium graminearum* species complex." *Fungal Genetics and Biology* 42, no. 5 (2005): 420-433.

Manes, Nimrat, Elizabeth K. Brauer, Shelley Hepworth, and Rajagopal Subramaniam. "MAMP and DAMP signalling contributes resistance to *Fusarium graminearum* in Arabidopsis." *Journal of Experimental Botany* 72, no. 18 (2021): 6628-6639.

McCormick, S. P., N. J. Alexander, and L. J. Harris. "CLM1 of *Fusarium graminearum* encodes a longiborneol synthase required for culmorin production." *Applied and environmental microbiology* 76, no. 1 (2010): 136-141.

Medema, Marnix H., Renzo Kottmann, Pelin Yilmaz, Matthew Cummings, John B. Biggins, Kai Blin, Irene De Bruijn et al. "Minimum information about a biosynthetic gene cluster." *Nature chemical biology* 11, no. 9 (2015): 625-631.

Mentges, Michael, Anika Glasenapp, Marike Boenisch, Sascha Malz, Bernard Henrissat, Rasmus JN Frandsen, Ulrich Güldener et al. "Infection cushions of *Fusarium graminearum* are fungal arsenals for wheat infection." *Molecular Plant Pathology* 21, no. 8 (2020): 1070-1087.

Merhej, Jawad, Florence Richard-Forget, and Christian Barreau. "The pH regulatory factor Pac1 regulates Tri gene expression and trichothecene production in *Fusarium graminearum*." *Fungal Genetics and Biology* 48, no. 3 (2011): 275-284.

Miller, Gad, Karen Schlauch, Rachel Tam, Diego Cortes, Miguel A. Torres, Vladimir Shulaev, Jeffery L. Dangl, and Ron Mittler. "The plant NADPH oxidase RBOHD mediates rapid systemic signalling in response to diverse stimuli." *Science signalling* 2, no. 84 (2009): ra45-ra45.

Miller, J. D., A. W. Schaafsma, D. Bhatnagar, G. Bondy, I. Carbone, L. J. Harris, G. Harrison et al. "Mycotoxins that affect the North American agri-food sector: state of the art and directions for the future." *World Mycotoxin Journal* 7, no. 1 (2014): 63-82.

Montibus, Mathilde, Christine Ducos, Marie-Noelle Bonnin-Verdal, Jorg Bormann, Nadia Ponts, Florence Richard-Forget, and Christian Barreau. "The bZIP transcription factor Fgap1 mediates oxidative stress response and trichothecene biosynthesis but not virulence in *Fusarium graminearum*." *PLoS One* 8, no. 12 (2013): e83377.

Morales, Jorge, Yasuhiro Kadota, Cyril Zipfel, Antonio Molina, and Miguel-Angel Torres. "The Arabidopsis NADPH oxidases RbohD and RbohF display differential expression patterns and contributions during plant immunity." *Journal of Experimental Botany* 67, no. 6 (2016): 1663-1676.

Nasmith, Charles G., Sean Walkowiak, L. I. Wang, Winnie WY Leung, Yunchen Gong, Anne Johnston, Linda J. Harris, David S. Guttman, and Rajagopal Subramaniam. "Tri6 is a global transcription regulator in the phytopathogen *Fusarium graminearum*." *PLoS pathogens* 7, no. 9 (2011): e1002266.

Nazari, Leyla, E. Pattori, Sara Somma, Valentina Manstretta, C. Waalwijk, A. Moretti, G. Meca, and Vittorio Rossi. "Infection incidence, kernel colonisation, and mycotoxin accumulation in durum wheat inoculated with *Fusarium sporotrichioides*, *F. langsethiae* or *F. poae* at different growth stages." *European Journal of Plant Pathology* 153, no. 3 (2019): 715-729.

Newman, Mari-Anne, Thomas Sundelin, Jon T. Nielsen, and Gitte Erbs. "MAMP (microbe-associated molecular pattern) triggered immunity in plants." *Frontiers in plant science* 4 (2013): 139.

Obanor, F., S. Neate, S. Simpfendorfer, R. Sabburg, P. Wilson, and S. Chakraborty. "*Fusarium graminearum* and Fusarium pseudograminearum caused the 2010 head blight epidemics in Australia." *Plant Pathology* 62, no. 1 (2013): 79-91.

O'Brien, Jose A., Arsalan Daudi, Paul Finch, Vernon S. Butt, Julian P. Whitelegge, Puneet Souda, Frederick M. Ausubel, and G. Paul Bolwell. "A peroxidase-dependent apoplastic oxidative burst in cultured Arabidopsis cells functions in MAMP-elicited defense." *Plant Physiology* 158, no. 4 (2012): 2013-2027.

Oide, Shinichi, Wolfgang Moeder, Stuart Krasnoff, Donna Gibson, Hubertus Haas, Keiko Yoshioka, and B. Gillian Turgeon. "NPS6, encoding a nonribosomal peptide synthetase involved in siderophore-mediated iron metabolism, is a conserved virulence determinant of plant pathogenic ascomycetes." *The plant cell* 18, no. 10 (2006): 2836-2853.

Oide, Shinichi, Franz Berthiller, Gerlinde Wiesenberger, Gerhard Adam, and B. Gillian Turgeon. "Individual and combined roles of malonichrome, ferricrocin, and TAFC siderophores in *Fusarium graminearum* pathogenic and sexual development." *Frontiers in Microbiology* 5 (2015): 759.

Osborne, Lawrence E., and Jeffrey M. Stein. "Epidemiology of Fusarium head blight on small-grain cereals." *International journal of food microbiology* 119, no. 1-2 (2007): 103-108.

Ontario Crop IPM - Wheat." 2026. Accessed February 18. https://cropipm.omafra.gov.on.ca/en-ca/crops/wheat/diseases/d262410f-0861-4e9b-9f5e-8dd25e74f321.

Pasquali, Matias, Emmanuelle Cocco, Cédric Guignard, and Lucien Hoffmann. "The effect of agmatine on trichothecene type B and zearalenone production in *Fusarium graminearum, F. culmorum* and *F. poae*." *PeerJ* 4 (2016): e1672.

Pasquali, Matias, Marco Beyer, Antonio Logrieco, Kris Audenaert, Virgilio Balmas, Ryan Basler, Anne-Laure Boutigny et al. "A European database of *Fusarium graminearum* and *F. culmorum* trichothecene genotypes." *Frontiers in microbiology*7 (2016): 406.

Pestka, James J. "Deoxynivalenol: mechanisms of action, human exposure, and toxicological relevance." Archives of toxicology 84, no. 9 (2010): 663-679.

Pitorre, Delphine, Christel Llauro, Edouard Jobet, Jocelyne Guilleminot, Jean-Paul Brizard, Michel Delseny, and Eric Lasserre. "RLK7, a leucine-rich repeat receptor-like kinase, is required for proper germination speed and tolerance to oxidative stress in Arabidopsis thaliana." *Planta* 232, no. 6 (2010): 1339-1353.

Planted Firmly in Ontario's Economy | Ontario Agri-Food Innovation Alliance." 2026. Accessed February 18. https://www.uoguelph.ca/alliance/our-impact/commercialization/planted-firmly-ontario%E2%80%99s-economy.

Pogány, Miklós, Uta von Rad, Sebastian Grun, Anita Dongó, Alexandra Pintye, Philippe Simoneau, Gunther Bahnweg, Levente Kiss, Balázs Barna, and Jörg Durner. "Dual roles of reactive oxygen species and NADPH oxidase RBOHD in an Arabidopsis-Alternaria pathosystem." *Plant physiology* 151, no. 3 (2009): 1459-1475.

Ponts, Nadia, Laetitia Pinson-Gadais, Christian Barreau, Florence Richard-Forget, and Thérèse Ouellet. "Exogenous H2O2 and catalase treatments interfere with Tri genes expression in liquid cultures of *Fusarium graminearum*." *FEBS letters* 581, no. 3 (2007): 443-447.

Ponts, Nadia, Leslie Couedelo, Laetitia Pinson-Gadais, Marie-Noëlle Verdal-Bonnin, Christian Barreau, and Florence Richard-Forget. "*Fusarium* response to oxidative stress by H2O2 is trichothecene chemotype-dependent." *FEMS Microbiology Letters* 293, no. 2 (2009): 255-262.

Poppenberger, Brigitte, Franz Berthiller, Doris Lucyshyn, Tobias Sieberer, Rainer Schuhmacher, Rudolf Krska, Karl Kuchler, Josef Glössl, Christian Luschnig, and Gerhard Adam. "Detoxification of the *Fusarium* mycotoxin deoxynivalenol by a UDP-glucosyltransferase from Arabidopsis thaliana." *Journal of Biological Chemistry* 278, no. 48 (2003): 47905-47914.

Proctor, Robert H., Thomas M. Hohn, and Susan P. McCormick. "Reduced virulence of Gibberella zeae caused by disruption of a trichothecene toxin biosynthetic gene." *Molecular plant-microbe interactions: MPMI* 8, no. 4 (1995): 593-601.

Qi, Peng-Fei, Ya-Zhou Zhang, Cai-Hong Liu, Jing Zhu, Qing Chen, Zhen-Ru Guo, Yan Wang et al. "*Fusarium graminearum* ATP-binding cassette transporter gene FgABCC9 is required for its transportation of salicylic acid, fungicide resistance, mycelial growth and pathogenicity towards wheat." *International journal of molecular sciences* 19, no. 8 (2018): 2351.

Qiu, Han, Xu Zhao, Wenqin Fang, Huiming Wu, Yakubu Saddeeq Abubakar, Guo-dong Lu, Zonghua Wang, and Wenhui Zheng. "Spatiotemporal nature of *Fusarium graminearum*-wheat coleoptile interactions." *Phytopathology Research* 1, no. 1 (2019): 26.

Rivas, Felix Juan Martínez, Alisdair R. Fernie, and Fayezeh Aarabi. "Roles and regulation of the RBOHD enzyme in initiating ROS-mediated systemic signalling during biotic and abiotic stress." *Plant Stress* 11 (2024): 100327.

Rubartelli, Anna, and Michael T. Lotze. "Inside, outside, upside down: damage-associated molecular-pattern molecules (DAMPs) and redox." *Trends in immunology* 28, no. 10 (2007): 429-436.

Robinson, Mark D., Davis J. McCarthy, and Gordon K. Smyth. "edgeR: a Bioconductor package for differential expression analysis of digital gene expression data." *bioinformatics* 26, no. 1 (2010): 139-140.

Rokas, Antonis, Matthew E. Mead, Jacob L. Steenwyk, Huzefa A. Raja, and Nicholas H. Oberlies. "Biosynthetic gene clusters and the evolution of fungal chemodiversity." *Natural product reports* 37, no. 7 (2020): 868-878.

Roy, Abhijeet, Aiswarya Jayaprakash, Raja Rajeswary T, A. Annamalai, and P. T. V. Lakshmi. "Genome-wide annotation, comparison and functional genomics of carbohydrate-active enzymes in legumes infecting *Fusarium oxysporum* formae speciales." *Mycology* 11, no. 1 (2020): 56-70.

Sarowar, Sujon, Syeda T. Alam, Ragiba Makandar, Hyeonju Lee, Harold N. Trick, Yanhong Dong, and Jyoti Shah. "Targeting the pattern-triggered immunity pathway to enhance resistance to *Fusarium graminearum*." *Molecular plant pathology* 20, no. 5 (2019): 626-640.

Schenk, Sebastian T., and Adam Schikora. "Staining of callose depositions in root and leaf tissues." *Bio-protocol* 5, no. 6 (2015): e1429-e1429.

Seong, Kye-Yong, Matias Pasquali, Xiaoying Zhou, Jongwoo Song, Karen Hilburn, Susan McCormick, Yanhong Dong, Jin-Rong Xu, and H. Corby Kistler. "Global gene regulation by *Fusarium* transcription factors Tri6 and Tri10 reveals adaptations for toxin biosynthesis." *Molecular microbiology* 72, no. 2 (2009): 354-367.

Shostak, Kristina, Christopher Bonner, Amanda Sproule, Indira Thapa, Samuel WJ Shields, Barbara Blackwell, John Vierula, David Overy, and Rajagopal Subramaniam. "Activation of biosynthetic gene clusters by the global transcriptional regulator TRI6 in *Fusarium graminearum*." *Molecular Microbiology* 114, no. 4 (2020): 664-680.

Sieber, Christian MK, Wanseon Lee, Philip Wong, Martin Münsterkötter, Hans-Werner Mewes, Clemens Schmeitzl, Elisabeth Varga, Franz Berthiller, Gerhard Adam, and Ulrich Güldener. "The *Fusarium graminearum* genome reveals more secondary metabolite gene clusters and hints of horizontal gene transfer." *PLoS One* 9, no. 10 (2014): e110311.

Smakowska-Luzan, Elwira, G. Adam Mott, Katarzyna Parys, Martin Stegmann, Timothy C. Howton, Mehdi Layeghifard, Jana Neuhold et al. "An extracellular network of Arabidopsis leucine-rich repeat receptor kinases." *Nature* 553, no. 7688 (2018): 342-346.

Sørensen, Jens Laurids, Frederik Teilfeldt Hansen, Teis Esben Sondergaard, Dan Staerk, T. Verne Lee, Reinhard Wimmer, Louise Graabæk Klitgaard, Stig Purup, Henriette Giese, and Rasmus John Normand Frandsen. "Production of novel fusarielins by ectopic activation of the polyketide synthase 9 cluster in *Fusarium graminearum*." *Environmental Microbiology* 14, no. 5 (2012): 1159-1170.

Sørensen, Jens Laurids, Teis Esben Sondergaard, Lorenzo Covarelli, Patricia Romans Fuertes, Frederik Teilfeldt Hansen, Rasmus John Normand Frandsen, Wagma Saei et al. "Identification of the biosynthetic gene clusters for the lipopeptides fusaristatin A and W493 B in *Fusarium graminearum* and *F. pseudograminearum*." *Journal of natural products* 77, no. 12 (2014): 2619-2625.

Spanic, Valentina, Marija Viljevac Vuletic, Ivan Abicic, and Tihana Marcek. "Early response of wheat antioxidant system with special reference to Fusarium head blight stress." *Plant physiology and biochemistry* 115 (2017): 34-43.

Su, Zhenqi, Amy Bernardo, Bin Tian, Hui Chen, Shan Wang, Hongxiang Ma, Shibin Cai et al. "A deletion mutation in TaHRC confers Fhb1 resistance to Fusarium head blight in wheat." *Nature genetics* 51, no. 7 (2019): 1099-1105.

Sun, Yadong, Lei Li, Alberto P. Macho, Zhifu Han, Zehan Hu, Cyril Zipfel, Jian-Min Zhou, and Jijie Chai. "Structural basis for flg22-induced activation of the Arabidopsis FLS2-BAK1 immune complex." *Science* 342, no. 6158 (2013): 624-628.

Tan, Jiang, Noémie De Zutter, Sarah De Saeger, Marthe De Boevre, Trang Minh Tran, Theo Van der Lee, Cees Waalwijk et al. "Presence of the weakly pathogenic *Fusarium poae* in the Fusarium head blight disease complex hampers biocontrol and chemical control of the virulent *Fusarium graminearum* pathogen." *Frontiers in Plant Science* 12 (2021): 641890.

Tang, Zhijun, Haoyu Tang, Wanqiu Wang, Yufeng Xue, Dandan Chen, Weihua Tang, and Wen Liu. "Biosynthesis of a new fusaoctaxin virulence factor in *Fusarium graminearum* relies on a distinct path to form a guanidinoacetyl starter unit priming nonribosomal octapeptidyl assembly." *Journal of the American Chemical Society* 143, no. 47 (2021): 19719-19730.

Team, R. Core. "RA language and environment for statistical computing, R Foundation for Statistical." *Computing* (2020).

Tobiasen, Carsten, Johan Aahman, Kristine Slot Ravnholt, Morten Jannik Bjerrum, Morten Nedergaard Grell, and Henriette Giese. "Nonribosomal peptide synthetase (NPS) genes in

Fusarium graminearum, F. culmorum and *F. pseudograminearium* and identification of NPS2 as the producer of ferricrocin." *Current genetics* 51, no. 1 (2007): 43-58.

Torres, Miguel Angel, Jonathan DG Jones, and Jeffery L. Dangl. "Pathogen-induced, NADPH oxidase–derived reactive oxygen intermediates suppress spread of cell death in Arabidopsis thaliana." *Nature genetics* 37, no. 10 (2005): 1130-1134.

Torres, Miguel Angel, Jonathan DG Jones, and Jeffery L. Dangl. "Reactive oxygen species signalling in response to pathogens." *Plant physiology* 141, no. 2 (2006): 373-378.

Trail, Frances. "For blighted waves of grain: *Fusarium graminearum* in the postgenomics era." *Plant physiology* 149, no. 1 (2009): 103-110

Walter, Stephanie, Paul Nicholson, and Fiona M. Doohan. "Action and reaction of host and pathogen during Fusarium head blight disease." *New Phytologist* 185, no. 1 (2010): 54-66.

Wang, Ying, Xifeng Li, Baofang Fan, Cheng Zhu, and Zhixiang Chen. "Regulation and function of defense-related callose deposition in plants." *International Journal of Molecular Sciences* 22, no. 5 (2021): 2393.

Weber, Julia, Marta Vaclavikova, Gerlinde Wiesenberger, Maximilian Haider, Christian Hametner, Johannes Fröhlich, Franz Berthiller, Gerhard Adam, Hannes Mikula, and Philipp Fruhmann. "Chemical synthesis of culmorin metabolites and their biologic role in culmorin and acetyl-culmorin treated wheat cells." *Organic & biomolecular chemistry* 16, no. 12 (2018): 2043-2048.

Westphal, Klaus Ringsborg, Katrine Amalie Hamborg Nielsen, Rasmus Dam Wollenberg, Mathias Bonde Møllehøj, Simone Bachleitner, Lena Studt, Erik Lysøe et al. "Fusaoctaxin A, an example of a two-step mechanism for non-ribosomal peptide assembly and maturation in fungi." *Toxins* 11, no. 5 (2019): 277.

Wipfler, Rebecca, Susan P. McCormick, Robert H. Proctor, Jennifer M. Teresi, Guixia Hao, Todd J. Ward, Nancy J. Alexander, and Martha M. Vaughan. "Synergistic phytotoxic effects of culmorin and trichothecene mycotoxins." *Toxins* 11, no. 10 (2019): 555.

Woelflingseder, Lydia, Benedikt Warth, Immina Vierheilig, Heidi Schwartz-Zimmermann, Christian Hametner, Veronika Nagl, Barbara Novak et al. "The *Fusarium* metabolite culmorin suppresses the in vitro glucuronidation of deoxynivalenol." *Archives of Toxicology* 93, no. 6 (2019): 1729-1743.

Wollenberg, Rasmus Dam, Wagma Saei, Klaus Ringsborg Westphal, Carina Sloth Klitgaard, Kare Lehmann Nielsen, Erik Lysøe, Donald Max Gardiner, Reinhard Wimmer, Teis Esben Sondergaard, and Jens Laurids Sørensen. "Chrysogine biosynthesis is mediated by

a two-module nonribosomal peptide synthetase." *Journal of Natural Products* 80, no. 7 (2017): 2131-2135.

Yan, W., H. B. Li, S. B. Cai, H. X. Ma, G. J. Rebetzke, and C. J. Liu. "Effects of plant height on type I and type II resistance to fusarium head blight in wheat." *Plant Pathology* 60, no. 3 (2011): 506-512.

Yu, Xiao, Baomin Feng, Ping He, and Libo Shan. "From chaos to harmony: responses and signalling upon microbial pattern recognition." *Annual review of phytopathology* 55, no. 1 (2017): 109-137.

Zhang, Wentao, Kerry Boyle, Anita Brule-Babel, George Fedak, Peng Gao, Zeinab Robleh Djama, Brittany Polley et al. "Evaluation of genomic prediction for Fusarium head blight resistance with a multi-parental population." Biology 10, no. 8 (2021): 756.

Zheng, Dawei, Shijie Zhang, Xiaoying Zhou, Chenfang Wang, Ping Xiang, Qian Zheng, and Jin-Rong Xu. "The FgHOG1 pathway regulates hyphal growth, stress responses, and plant infection in *Fusarium graminearum*." *PloS one* 7, no. 11 (2012): e49495.

Supplemental Data

Supplementary Data 1: Time course transcriptomic analysis of *F. graminearum* infected in WT Arabidopsis seedlings.

Supplemental 1A: Differentially expressed *F. graminearum* genes at 2 dpi during Arabidopsis seedling infection (relative to 1 dpi).

Supplemental 1B: Differentially expressed *F. graminearum* genes at 3 dpi during Arabidopsis seedling infection (relative to 1 dpi).

Supplemental 1C: Differentially expressed *F. graminearum* genes at 4 dpi during Arabidopsis seedling infection (relative to 1 dpi).

Supplemental 1D: GO term enrichment analysis of 2 dpi DEGs in *F. graminearum* during Arabidopsis seedling infection.

Supplemental 1E: GO term enrichment analysis of 3 dpi DEGs in *F. graminearum* during Arabidopsis seedling infection.

Supplemental 1F: GO term enrichment analysis of 4 dpi DEGs in *F. graminearum* during Arabidopsis seedling infection.

Supplemental 1G: GO enrichment of DEGs shared across 2-4 dpi

Supplemental 1H: Differentially expressed *F. graminearum* genes shared across 2–4 dpi during Arabidopsis infection

Supplemental 1I: BGC and DEG expression uniquely enriched at 4 dpi in *F. graminearum* during Arabidopsis infection.

Supplemental 1J: Differentially expressed CAZymes in *F. graminearum* during Arabidopsis seedling infection (2-4 dpi).

Supplementary Data 2: Transcriptomic analysis of *F. graminearum* infected in Arabidopsis **WT and *rbohD* seedlings.**

Supplementary Data 2A: Differentially expressed *F. graminearum* genes with increased expression in infected *rbohD* relative to WT plants.

Supplemental Data 2B: Differentially expressed *F. graminearum* genes with reduced expression in infected *rbohD* relative to WT plants.

Supplemental Data 2C: Gene ontology (GO) enrichment analysis of *F. graminearum* genes with higher expression in infected *rbohD* relative to WT plants.

Supplemental Data 2D: Gene ontology (GO) enrichment analysis of *F. graminearum* genes with lower expression in infected *rbohD* relative to WT plants.

Supplemental Data 2E: *F. graminearum* predicted CAZymes with differential expression in infected *rbohD* relative to WT plants.

Supplemental Figures

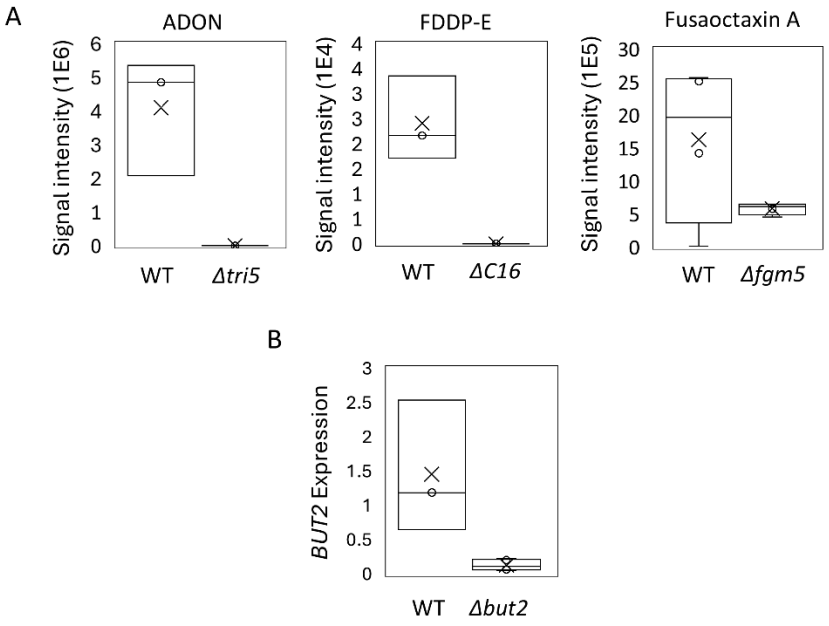

Figure S1. Confirmation of knockout production in different *F. graminearum* mutants.

A) The boxplot represents confirmation of knockout production of each *F. graminearum* mutant using metabolomics. Arabidopsis WT Col-0 seedlings inoculated with *F. graminearum* DAOM233423, *Δtri5, Δfgm5* and *ΔC16* were harvested 4 dpi (n=4). The experiment was repeated once.

B) The boxplot represents confirmation of knockout production of each *F. graminearum* mutant using qPCR. Arabidopsis WT *rbohD* mutant seedlings inoculated with *F. graminearum* DAOM233423 and *Δbut2* were harvested 3 dpi (n=6). The ratio of fungal gene expression relative to fungal housekeeping genes (*GAPDH, Fg β-tubulin*).

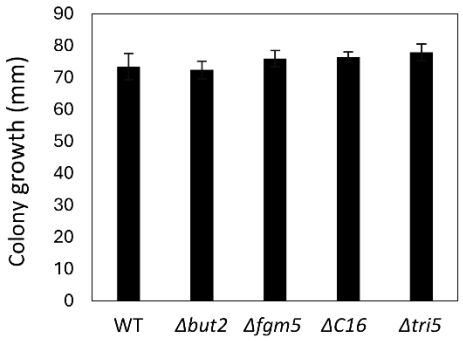

Figure S2. Colony growth of wild type and *F. graminearum* mutant strains on PDA. *F. graminearum* spores were inoculated on potato dextrose agar (PDA) and incubated at 25°C for 5 days (n=5). All strains showed similar colony diameters with no statistically significant differences between WT and *F. graminearum* mutants stains, indicating that the mutation doesn't not affect growth under high nutrient conditions. The experiment was repeated three times and the data from one experiment is plotted here.

Supplemental Tables

Supplementary Table S1. List of primers used in this study.

Gene	Gene ID	Forward (5' --> 3')	Reverse (5' --> 3')
PP2A	*AT1G69960*	AGTTCCAGAATCCAAACCAAC	CCTAGAGGCAACACAAACATC
Plant β-tubulin	*AT4G14960*	GGTCAATACGTCGGCGATTC	TCTGACCGAACGGACCAGAT
BIK1	*AT2G39660*	GGTGGCTTTGGTTGTGTCTT	CACGGTGACCTTGAAAACCT
GAPDH	*FGSG_16627*	TGACTTGACTGTTCGCCTCGA	ATGGAGGAGTTGGTGTTGCC
β-Tubulin	*FGSG_09530*	CATGCAAATGTCGTAGAGGG	GTTGATCTCCAAGATCCGTG
TRI3	*FGSG_03534*	CACCCTTGGTACCAGCACTT	CTCTTCCAGTCCAACAATTGCC
TRI5	*FGSG_03537*	GGCCCAAGGACCTGTTTGAT	CAACGGCTGACGTGATTTCA
TRI6	*FGSG_03536*	CATCGTCGGGACTGTGGA	AAGGTGGGAAGGGCGATAA
TRI9	*FGSG_03539*	GCGGGGATCTTCACAAGGAA	CGAATCAGTGCTGTGTCCCT
NRPS8	*FGSG_11659*	CTCGCATAGCATACCTACATCAA	CGAGATGAGCGAGAAGAAGAAG
NRPS9	*FGSG_10990*	TTTGGGCCATGTCACTCCTC	CCGCCACGGCTAATTTGATG
Fgm5	*FGSG_10995*	CGACAATTCCTTTGGCCCGA	ACGAGTGAGTGCTAGCAGGA
But2	*FGSG_08080*	TCCGCGAACCTGACAATAGG	TTGTATTGCTGGGAGGGCTG
Clm1	*FGSG_10397*	TTGTGGCTCGCAAGGGTATT	TCCAGGTTGGGGAATTGTCG
n/a	*FGSG_04591*	ATCCACAGCATCCGCTCAAA	GCAATGCTCGAATGAGCCAG
n/a	*FGSG_04596*	GCCAGGAACCATTGACATGC	TCCAACCCAGTCTGCTTCAC

*n/a, no annotated gene name

Table S2. Proportion of *F. graminearum* inoculated Arabidopsis seedlings which exhibit H_2O_2 production in 4 different tissues. Arabidopsis WT and mutants (*rbohD, apex-1, rlk7-4 & ilk1-1*) seedlings inoculated with *F. graminearum* DAOM233423 were harvested 3 dpi. In addition, Arabidopsis WT Col-0 were inoculated with *ΔnoxA/B*. This experiment was repeated 4 times with similar results. Infection with the *ΔnoxA/B* strain and uninfected WT seedlings were repeated twice.

Genotype	Seedlings with DAB	Seedlings with no DAB	Seedling number	% with DAB
Cotyledon				
WT	66	2	68	97
WT uninfected	2	9	13	15
rbohD	3	45	48	6
ilk1-1	33	11	44	75
apex-1	34	13	47	72
rlk7-1	38	25	63	60
WT (*Δnoxa/b)*	11	0	11	100
Stem				
WT	42	26	68	62
WT uninfected	1	12	13	8
rbohD	0	48	48	0
ilk1-1	13	31	44	30
apex-1	21	26	47	45
rlk7-1	23	40	63	37
WT (*Δnoxa/b)*	9	2	11	82
Root tip				
WT	40	28	68	59
WT uninfected	5	8	13	38
rbohD	13	35	48	27
ilk1-1	11	33	44	25
apex-1	2	45	47	4
rlk7-1	8	55	63	13
WT (*Δnoxa/b)*	0	11	11	0
Root Cortex				
WT	65	3	68	96
WT uninfected	13	0	13	100
rbohD	37	11	48	77
ilk1-1	38	6	44	86

apex-1	41	6	47	87
rlk7-1	63	0	63	100
WT (*Δnoxa/b)*	6	6	12	50

Table S3. Trypan blue staining quantification of cotyledon in Arabidopsis seedlings infected with *F. graminearum*. Arabidopsis WT and *rbohD* seedlings inoculated with *F. graminearum* DAOM233423 were harvested 3 dpi. Cotyledons were scored for the presence or absence of trypan blue staining. This experiment was repeated twice with similar results. The data from all experiments is shown.

Genotype	**Seedlings with cell death**	**Seedlings with no cell death**	**Seedling number**	**% of cell death**
WT uninfected	2	12	14	14
rbohD uninfected	3	11	14	21
WT	54	1	55	98
rbohD	36	6	42	86